International Journal of Water Resources and Environmental Engineering

Volume 9 Number 8 August 2017

ISSN-2141-6613

Academic Journals

ABOUT IJWREE

The International Journal of Water Resources and Environmental Engineering is published monthly (one volume per year) by Academic Journals.

International Journal of Water Resources and Environmental Engineering (IJWREE) is an open access journal that provides rapid publication (monthly) of articles in all areas of the subject such as water resources management, waste management, ozone depletion, Kinetic Processes in Materials, strength of building materials, global warming etc. The Journal welcomes the submission of manuscripts that meet the general criteria of significance and scientific excellence. Papers will be published shortly after acceptance. All articles published in IJWREE are peer-reviewed.

Contact Us

Editorial Office: ijwree@academicjournals.org

Help Desk: helpdesk@academicjournals.org

Website: http://www.academicjournals.org/journal/IJWREE

Submit manuscript online http://ms.academicjournals.me/

Editorial Board

International Journal of Water Resources and Environmental Engineering

Table of Contents: Volume 9 Number 8 August 2017

ARTICLES

Evaluation of empirical models for estimating reference-evapotranspiration (RET-ET) in humid semihot equatorial coastal climate 162
Itolima Ologhadien and Ify L. Nwaogazie

Analysis of spatial and temporal drought variability in a tropical river basin using Palmer Drought Severity Index (PDSI) 178
Raphael M. Wambua, Benedict M. Mutua and James M. Raude

academicJournals

Vol. 9(8), pp. 162-177, August 2017
DOI: 10.5897/IJWREE2017.0731
Article Number: C791CF265325
ISSN 2141-6613

http://www.academicjournals.org/IJWREE

International Journal of Water Resources and Environmental Engineering

Full Length Research Paper

Evaluation of empirical models for estimating reference-evapotranspiration (RET-ET) in humid semi-hot equatorial coastal climate

Itolima Ologhadien[1] and Ify L. Nwaogazie[2]*

[1]Department of Civil Engineering, Rivers State University of Science and Technology, Nkpolu, Port Harcourt, Nigeria.
[2]Department of Civil and Environmental Engineering, University of Port Harcourt, Nigeria.

Received 6 June, 2017; Accepted 10 July, 2017

The performances of five empirical models, namely: Hargreaves-Samani, Makkink1 (1957), Makkink2 (1984), Priestley-Taylor and FAO 56-PM in estimating reference evapotranspiration (REF-ET) were separately compared with Epan data and FAO 56-PM, respectively. Based on statistical analysis, Hargreaves-Samani method compared best with daily and monthly Epan data, while Makkik2 (1984) ranked first with FAO 56-PM. In terms of regression analysis, Priestley-Taylor performed best with daily FAO 56-PM method while Hargreaves-Samani ranked first with daily Epan data. Hargreaves-Samani also correlated best with mean monthly Epan data. The quantitative evaluation of cumulative daily and monthly reference-evapotranspiration (RET-ET) values showed that Makkink (1984) produced the least overestimation and percent relative error against FAO 56-PM while Hargreaves-Samani performed best with Epan data with the least overestimation and percent relative error. In terms of cumulative monthly ET_o totals for the farming season (Dec-April) over the study period, Hargreaves-Samani ranked best with Epan data with the least overestimation and percent relative error while Priestley–Taylor ranked best with FAO 56-PM producing the least overestimation. Overall, Hargreaves-Samani with its original coefficient was adjudged best, capable of approximating FAO 56-PM and Epan data in the Lower Niger River Basin, followed by Makkink (1984) and Priestley-Taylor. Penman-Monteith estimates were used to develop monthly correction factors for adjusting Empirical models for their potential use in Lower Niger Basin. A comparative study such as this has not been undertaken in the Lower Niger River Basin. The models recommended in this study are economical, lesser-data demanding and can be applied to predicting REF-ET in remote agricultural areas.

Key words: Reference-evapotranspiration (RET-ET), empirical models, radiation-based methods, temperature-based methods, FAO 56 –PM, Lower Niger River Basin.

INTRODUCTION

The accurate knowledge of evapotranspiration and consumptive use of water is an index of successful food production programme. The availability of water and efficiency of its economic use are dominant factors controlling or limiting food production and a better understanding of water requirements can, therefore result in large benefits (Hargreaves and Samani, 1981). Irrigation water demand is usually determined through evapotranspiration estimation procedures, namely; (i) direct field measurement methods such as Lysimeter

apparatus and US weather Bureau Standard Class A pan and (ii) empirical relationships and mathematical model based on weather data to determine Reference Evapotranspiration (REF-ET) (Jensen et al., 1990; Allen et al., 1998). The Lysimeter apparatus, and Evaporation pans with associated automated measurement devices are rather expensive and are located at a limited number of weather stations around the United States and the world (William et al., 2008). In developing countries like Nigeria, there are additional problems of poor staffing, lack of regular site visitation, improper equipment calibration and instrument.

In view of the human resources and costs implications of using direct measurement methods, empirical and mathematical models based on weather data have become an attractive alternative.

The concept of reference evapotranspiration, REF-ET was introduced to model the evaporative demand of the atmosphere independent of crop type, crop development and management practices. Consequently, REF-ET values measured or calculated at different locations or in different seasons are comparative as they refer to the evapotranspiration (ET_o), from the same reference surface (Allen et al., 1998). The empirical models for evaluation of REF-ET can be grouped into five categories namely: i) water budget, ii) Mass-transfer, iii) Combination, iv) Radiation-based, and v) Temperature based.

The availability of numerous equations for determination of ET, the wide range of data types needed, and the wide range of expertise needed to use the various equations correctly make it difficult to select the most appropriate evaporation method for a given study location (Xu and Singh, 2002). Therefore, the most appropriate method for a given geographical location is to be found by research on comparative studies. In the humid semi-hot equatorial climate of the lower Niger basin, comparative studies with the objective of selecting the best ET_o model are lacking. The aim of this study, therefore, was to evaluate five frequently referred ET_o models (Table 1) and compare them first against Epan data and secondly against FAO 56-PM (where PM stands for Penman-Monteith equation). The daily and monthly REF – ET values were calculated following examples 17 and 18, of Allen et al. (1998) on pages 70 to 73 as guide. The calculation procedures outlined in examples 17 and 18 with the sample data were first programmed in Excel spreadsheet. After the Excel calculations had accurately reproduced the results of example problems, then the example data were replaced with the study data. The study data were the routinely measured variables, maximum temperature (T_{max}), minimum temperature (T_{min}), mean temperature (T_{mean}), measured solar radiation (Rs), relative humidity (RH), wind speed (u_2), and z only (where z is the elevation of the site in metres).

This study will be of great economic benefits to Nigeria, in view of the declining oil and gas revenues and the shift to agricultural economy. Most of the agricultural and allied industries are situated in remotest area without weather stations. The result of this study would be the recommendation of an empirical and less weather-data demanding REF-ET equation to FAO 56-PM which can easily be applied to such locations.

MATERIALS AND METHODS

Weather station

The weather station used in this study is located at the Port Harcourt International Airport, Omagwa, Rivers State, Nigeria. The station is located at latitude 04°51'N and longitude 05°35'E, elevation of 24 m (above sea level). The Nigerian Meteorological Agency (NIMET) station is equipped with the mercury and alcohol thermometers, a cup anemometer, a Campbell sunshine recorder, and a wet-bulb thermometer and some other meteorological instruments. All the instruments were checked for proper installation and operation during observations by NIMET. Figure 1 is the map of Lower Niger River Basin showing Port Harcourt while Table 2 shows the mean monthly weather characteristics for the study period. The climate of Port Harcourt may be classified as Humid Semi – Hot Equatorial Type (Salau and Lawson, 1986), with tropical wet and dry season and pronounced seasonal reversal of wind directions. The annual rainfall is greater than 3000 mm. The wet season occurs between March and October and dry season from November to February, sometimes with occasional rainfall.

Description of empirical equations

Penman-Monteith method

The FAO Penman-Monteith method is physically based, and explicitly incorporates both physiological and aerodynamic parameters (Allen et al., 1998). The form of FAO 56-PM equation for predicting ET_o on a daily basis is:

$$ET_o = \frac{0.408\Delta(R_n - G) + \gamma \frac{900}{T+273} U_2 (e_S - e_a)}{\Delta + \gamma(1 + 0.34 U_2)} \quad (1)$$

Where ET_o is the reference evapotranspiration ($mmday^{-1}$), Δ is slope of the vapour pressure curve ($kPa\ °C^{-1}$), R_n is net radiation at the crop surface ($MJm^{-2}day^{-1}$); G is soil heat flux density ($MJm^{-2}day^{-1}$); T is air temperature (°C) at 2 m height, U_2 is wind speed at 2 m height (ms^{-1}), e_s = saturation vapour pressure (kPa), e_a is actual vapour pressure (kPa), γ is psychometric constant ($kPa\ °C^{-1}$), and $e_s - e_a$ is saturation vapour pressure deficit (kPa). The complementary parameters λ, P, e_s, e_a, Δ, and γ have been calculated following the procedures given in Chapter 3 of FAO 56 (Allen et al., 1998). For

*Corresponding author. E-mail: ifynwaogazie@yahoo.com.

Table 1. Characteristics of REF-ET methods (adapted from Amatya et al., 1995).

Empirical models	Main parameter required ±	Recommended time period	Reference crop	Location developed for	Principal reference
FAO 56-PM Penman Monteith	Temp., rel.hum., Net solar rad., Rn	Hourly, daily, weekly, monthly	Any Crop	All Locations	Jensen et al. (1990); Allen et al. (1994a, b; 1998)
Makkink1 (1957) Makkink2 (1984)	Temperature, incoming solar Rad (R_S)	10 days, monthly	Grass	Cool climate, the Netherlands, Australia	Jensen (1974), Jensen et al. (1990); Xu and Singh (2000)
Priestley-Taylor (1972)	Temperature (T) net radiation (R_n)	10 days, monthly	Rain – fed Land	Australia, United States	Jensen et al. (1990); Xu and Singh (2000)
Hargreaves-Samani	T_{max}, T_{min}, T_{mean} extraterrestrial Radiation (Ra)	Weekly, Monthly	Cool – season grass	Semiarid Western US	Jensen et al. (1990); Xu and Singh (2001)

± The appropriate units for the main parameters are given in Equations 1 – 10.

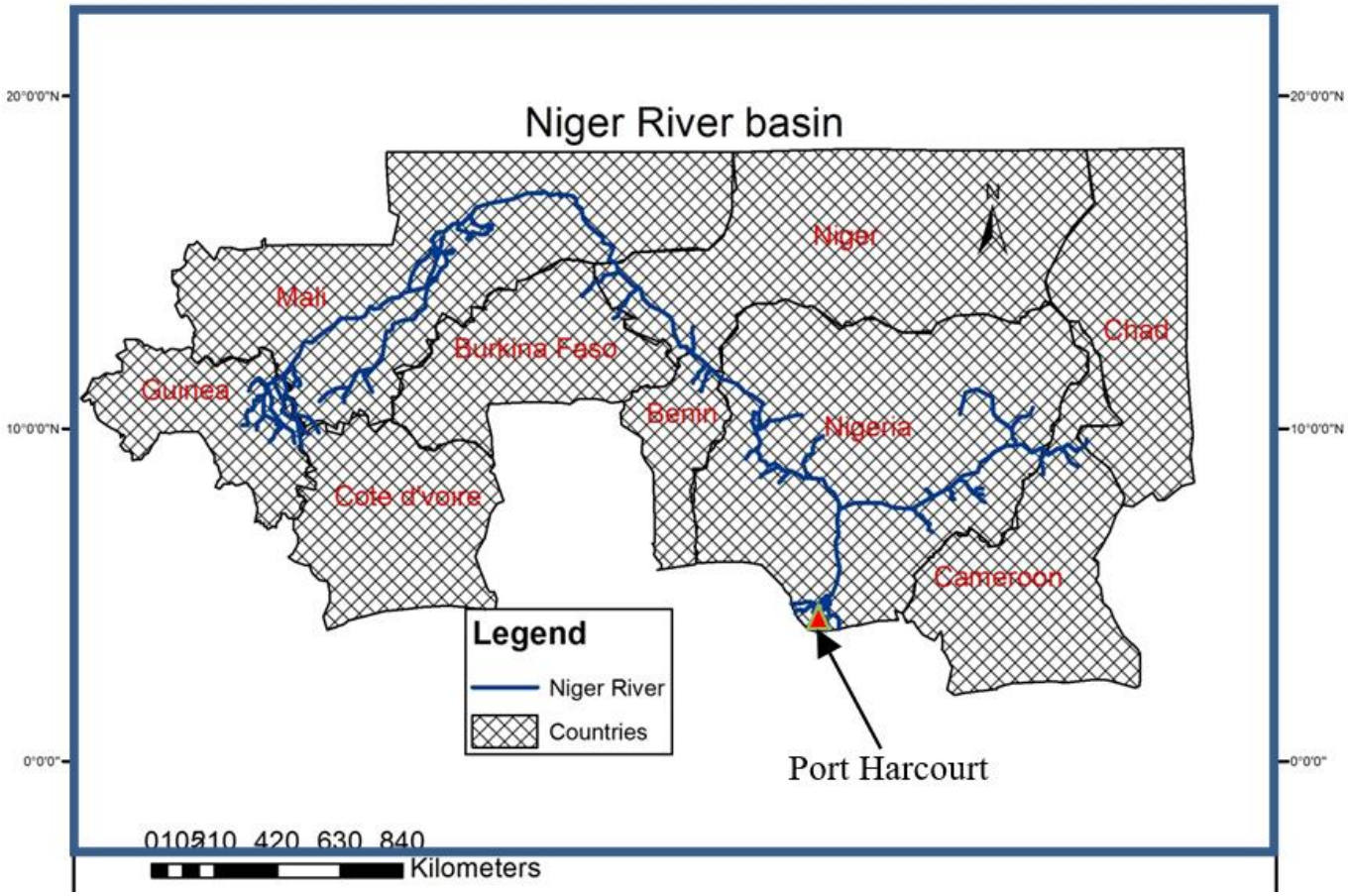

Figure 1. Map of the Niger River Basin Showing Port Harcourt.

the sake of completeness, other important parameters are briefly summarized below:

Net longwave radiation ($R_{n\ell}$): The rate of longwave energy emission may be expressed quantitatively by the Stefan-Boltzman constant due to the absorption and downward radiation from the sky as:

$$R_{n\ell} = \sigma\left[\frac{T_{\max},K^4 + T_{\min},K^4}{2}\right]\left(0.34 - 0.14\sqrt{e_a}\right)\left(1.35\frac{R_s}{R_{so}} - 0.35\right) \quad (2)$$

Table 2. Daily averages of selected climatic parameters (2000-2010).

Parameters / Month	U_2 (m/s)	Tmax (°C)	Tmean (°C)	Mean RH	Solar Rad.	Barometer pressure
Jan.	3.00	30.8	20.32	25.55	67.8	94.19
Feb.	3.30	31.1	20.93	26.01	67.57	92.03
Mar.	4.00	34.4	24.28	29.36	81.57	103.1
April	3.76	31.9	23.07	27.49	80.12	98.26
May	3.75	31.3	23.00	27.16	82.63	98.55
Jun	3.75	29.02	22.03	25.52	84.06	96.67
July	4.07	29.80	23.32	26.55	90.33	103.52
Aug.	3.91	29.3	23.28	26.28	90.5	103.06
Sept.	3.81	30.6	23.71	27.17	91.61	104.56
Oct.	3.21	30.1	22.57	26.34	85.00	99.20
Nov.	2.54	27.3	19.72	23.52	71.89	86.56
Dec.	2.38	27.92	18.95	23.44	65.61	86.06

Where $R_{n\ell}$ is net outgoing longwave radiation ($MJm^{-2}day^{-1}$), σ is Stefan-Boltzmann (4.903×10^{-9} $MJK^{-4}m^{-2}day^{-1}$); T_{max} is maximum absolute temperature during the 24 h period [K = °C + 273.16]; T_{min} is minimum absolute temperature during the 24 h period e_a is actual vapour pressure (kPa), $\frac{R_S}{R_{SO}}$ is relative short wave radiation (limited to ≤ 1.0); R_s is measured or calculated solar radiation ($MJm^{-2}day^{-1}$), R_{so} is calculated (Equation 3) clear-sky radiation ($MJK^{-4}m^{-2}day^{-1}$).

Short wave radiation on a clear-sky day (R_{so}): A good approximation for R_{so} according to FAO (Allen et al., 1998), for daily and hourly periods is given by Equation (3).

$$R_{so} = (0.75 + 2 \times 10^{-5} z) R_a \quad (3)$$

Where z is station elevation [m], R_a is extraterrestrial radiation [$MJm^{-2}day^{-1}$] and R_{so} is clear – sky solar radiation [$MJm^{-2}day^{-1}$].

Extraterrestrial radiation for daily periods (Ra): The extraterrestrial radiation (R_a), for each day of the year and for different latitude can be estimated from solar constant, the solar declination and the time of the year by:

$$R_a = \frac{24(60)}{\pi} G_{sc} \left[\omega_s Sin(\varphi) Sin(\delta) + Cos(\varphi) Cos(\delta) Sin(\omega_s) \right] \quad (4)$$

Where R_a = extraterrestrial radiation [$MJm^{-2}day^{-1}$], G_{sc} = solar constant = 0.0820 [$MJm^{-2}min^{-1}$], dr = Inverse relative distance Earth – sun, ω_s = sunset hour angle, φ = latitude (rad.), δ = Solar declination. The complimentary equations for calculating dr, ω_s, φ and δ are given in Allen (1996) or any standard text in hydrology.

Net short wave radiation (R_{ns}): The net shortwave radiation resulting from the balance between incoming and reflected solar radiation is given by:

$$R_{ns} = (1 - \alpha) R_s \quad (5)$$

Where R_{ns} = net shortwave radiation [$MJm^{-2}day^{-1}$]; α is = albedo, which is 0.23 for the hypothetical grass reference crop [dimensionless]; R_s = incoming solar radiation [$MJm^{-2}day^{-1}$] and R_{ns} is expressed in the above equation in $MJm^{-2}day^{-1}$.

Net radiation (R_n): The net radiation (R_n) is the difference between the incoming net short wave radiation (R_{ns}) and the outgoing net longwave radiation $(R_{n\ell})$.

$$R_n = \left(R_{ns} - R_{n\ell}\right) \quad (6)$$

Temperature-based equation

FAO-56 (Allen et al., 1998) recommended Hargreaves method as alternative approach when solar radiation, relative humidity and or wind speed data are missing. In the temperature-based category, the Hargreaves' equation has been selected.

$$ET_o = 0.0023 (T_{mean} + 17.8)(T_{max} - T_{min})^{0.5} R_a \quad (7)$$

Where ET_o = reference evapotranspiration (mmd^{-1}); R_a is extraterrestrial radiation [$MJm^{-2}day^{-1}$].

Radiation-based equations

Given Makkink (1984) and Priestley-Taylor (1972), two models have been selected in this study to represent the radiation-based method. Also, the lower Niger Delta region is similar to the Netherlands, where Makkink equation was found to give good results (Hansen, 1984); the two forms of Makkink equation and Priestley-Taylor are next discussed.

Makkink Method (1957) (Makkink1): The reference evapotranspiration (ET_o) according to Makkink (1957) is:

$$ET_o = 0.61 \frac{\Delta}{\Delta + \gamma} \cdot \frac{Rs}{\lambda} - 0.12 \quad (8)$$

Where R_s is solar radiation ($MJm^{-2}day^{-1}$); Δ is slope of saturation vapour pressure curve at the temperature T (kρa $°C^{-1}$), γ is psychrometric constant (kρa $°C^{-1}$), λ is latent heat of vapourization, 2.45 ($MJkg^{-1}$).

Makkink Method (1984) (Makkink 2):

$$ET_o = 0.7 * \frac{\Delta}{\Delta + \gamma}\frac{Rs}{\lambda} \quad (9)$$

ET_o, Δ, γ, Rs and λ are as defined under Equation 1.

Priestley-Taylor Method: The Priestley-Taylor method (1972) replaces the aerodynamic term of Penman-Monteith equation by a dimensionless empirical multiplier, called the Priestley- coefficient (α). The Priestley-Taylor equation is useful for the calculation of daily ET_o for conditions where weather input for the aerodynamic term (relative humidity, wind speed) are unavailable.

$$ET_o = \alpha \cdot \frac{\Delta}{\Delta + \gamma}.\frac{(R_n - G)}{\lambda} \quad (10)$$

Where ET_o is reference evapotranspiration (mm/day); α = 1.26, λ is the latent heat of vapourization [λ = 2.45 $MJkg^{-1}$ at 20°C]; and all other terms are the same as in Equation 1.

EVALUATION OF EMPIRICAL MODEL PERFORMANCE

Quantitative methods listed in Equations 11 to 18 have been used to test the strength of and/or weakness of the different models. These methods are indicators of model performance according to Fox (1981), Willmott (1982), Douglas et al. (2009), Berengena and Gavilan (2005), Alexandris et al. (2008), Pogen et al. (2016), and Dash and Khatua (2016). These statistical measures and the regression equations were evaluated using their optimal values as benchmarks.

i) Mean Absolute Error (MAE) = $$N^{-1}\sum_{i=1}^{N}|P_i - O_i| \quad (11)$$

ii) Root Mean Square Error (RMSE) = $$\left[N^{-1}\sum_{i=1}^{N}\left(P_i - O_i\right)^2\right]^{0.5} \quad (12)$$

iii) Root Mean Square Error (Systematic)(RMSEs) $$\left[N^{-1}\sum_{i=1}^{N}\left(\hat{P}_i - O_i\right)^2\right]^{0.5} \quad (13)$$

iv) Root Mean Square Error (unsystematic) (RMSEu) = $$\left[N^{-1}\sum_{i=1}^{N}\left(Pi - \hat{Pi}\right)^2\right]^{0.5} \quad (14)$$

v) Model efficiency (EF) = $$1 - \frac{\sum_{i=1}^{N}(P_i - O_i)^2}{\sum_{i=1}^{N}(\bar{O} - O_i)^2}$$; 0<=EF<= 1.0 (15)

vi) Mean Bias Error (MBE) = $$N^{-1}\sum_{i=1}^{N}\left(Pi - O_i\right) \quad (16)$$

vii) Variance of the distribution of differences $\left(S_d^2\right)$ = $$N-1\sum_{i=1}^{N}\left(P_i - O_i - MBE\right)^2 \quad (17)$$

viii) Index of Agreement (d) = 1 - $$\frac{\sum_{i=1}^{N}(P_i - O_i)^2}{\sum_{i=1}^{N}\left(|P_i| + |O_i|\right)^2}; 0 \le d \le 1.0 \quad (18)$$

The notations and indices used in Equations 11 to 18 are as follows:

O_i is observed values (estimated by FAO 56-PM or Epan), P_i is value predicted by any of the empirical equations used in the study, $\hat{P}_i = aO_i + b, P'_i = P_i - \bar{O}$ and, $O'_i = O_i - \bar{O}$.

RESULTS

The results of the study are summarized in Appendix A (Tables A1 and A2), Tables 3 and 4 and Figures 2 to 7. The first stage of analysis involved the estimation of mean daily and mean monthly evapotranspiration based on Equations (1, 7, 8, 9 and 10) with their original constants. Subsequent analyses involved evaluation of REF – ET methods against FAO 56-PM and Epan data using: i) statistical measures represented by Equations (11-18), ii) statistical regression analysis, and iii) total accumulated daily and monthly ET_o values and graphical plots. Tables A1 and A2 show the results of evaluation using Equations (11 to 18). In Tables A1 and A2, R represents the daily rank number for each statistical index while R^* represents the corresponding monthly rank number for each statistical index. The score for each ET_o method was obtained by adding the rank numbers under R or R^*.

The evaluation of daily and monthly ET_o estimates against Epan data are as presented in Table A1. The computed ET_o values for FAO 56-PM, Hargreaves-Samani, Makkink-1, Makkink-2, and Priestley – Taylor were ranked for each of the nine indices (see column 1, Appendix A, Table A1). The cumulative ranked values of R and R* are as shown in Figure 2. Apparently, the order of ranked performance are 1st Hargreaves-Samani, 2nd Makkink-2, 3rd Priestley-Taylor, 4th FAO 56-PM and 5th Makkink-1, respectively.

For the comparison of estimated ETo against ETo-PM for daily and monthly values (Appendix A, Table A2) The cumulative ranked values of R and R* (Figure 3) are 1st Makkink-2 with the lowest aggregate score; 2nd Epan; 3rd Makkink-1; 4th Priestley-Taylor; and 5th Hargreaves-Samani.

The summary of regression models of daily and monthly data are presented in Table 3. The goodness of fit of the correlation was adjudged by R^2, in addition to the slope (b) and intercept (c) of the regression line. The applicable linear probability model was obtained by

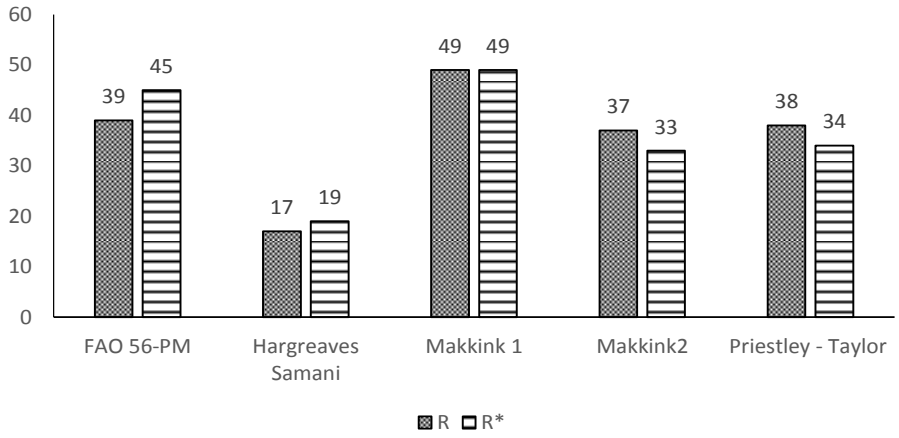

Figure 2. Comparison of cummulative ranking values of R & R* for estimated ET_o against Epan daily and monthly values.

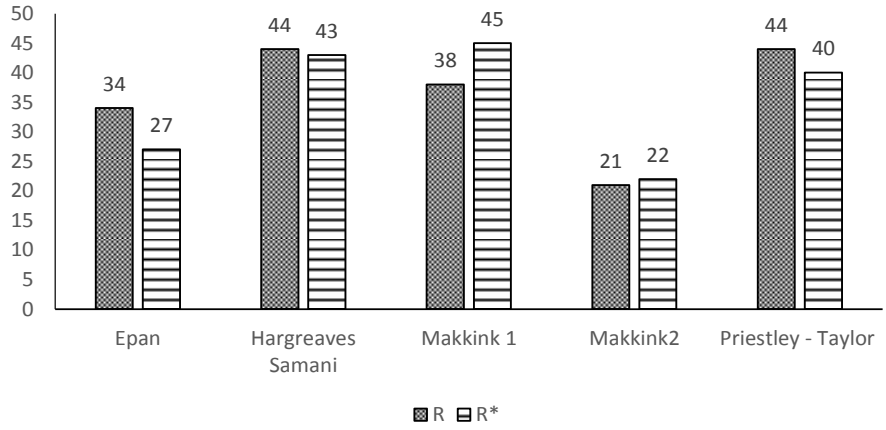

Figure 3. Comparison of cummulative ranking values of R & R* for estimated ET_o against ETo-PM daily and monthly values).

Table 3. Summary of linear regression equation against Epan/ET_o-PM.

S/N	a) Based on Daily Data		b) Based on Monthly Data		% Improvement on R^2 (daily and monthly)
	Equation Form	R^2	Equation Form	R^2	
1	ETo-PM = 0.636 Epan + 1.0663	0.443	ETo-PM = 0.948Epan - 0.188	0.785	77.2
2	ETo-PM = 0.644 ETo_{Harg} + 0.975	0.408	ETo-PM = 0.947ETo_{Harg} - 0.309	0.808	98.1
3	ETo-PM = 1.483 ETo_{MKK2} - 2.04	0.519	ETo-PM = 1.203ETo_{MKK2} - 0.84	0.771	25.2
4	ETo-PM = 1.075ETo_{RT} - 0.675	0.281	ETo-PM = 1.042 ETo_{P-T} - 0.484	0.636	126.3
5	ETo-PM = 1.702 ETo_{MKK1} - 1.84	0.519	ETo-PM = 1.416ETo_{MKK1} - 0.798	0.778	49.9
1	Epan = 0.696ETo_{PM} + 1.64	0.442	Epan = 0.827ETo_{PM} + 0.963	0.785	22.5
2	Epan = 0.9644 ETo_{Harg} + 0.0677	0.836	Epan = 0.945ETo_{Harg} + 0.078	0.922	10.3
3	Epan = 1.335 ETo_{MKK2} - 0.971	0.384	Epan = 1.050 ETo_{MKK2}+ 0.0752	0.674	43.0
4	Epan = 1.634 ETo_{Harg} - 0.545	0.30	Epan = 0.956 ETo_{P-T} + 0.2156	0.614	51.1
5	Epan = 1.532 ETo_{MKK1} – 0.788	0.384	Epan = 1.234 ETo_{MKK1} + 0.1186	0.678	43.4

regressing: (i) mean daily and mean monthly, ET_o-PM values against ET_o values, and (ii) mean daily and monthly Epan values against ET_o values. Both ET_o-PM and Epan data were used as comparison criteria. A

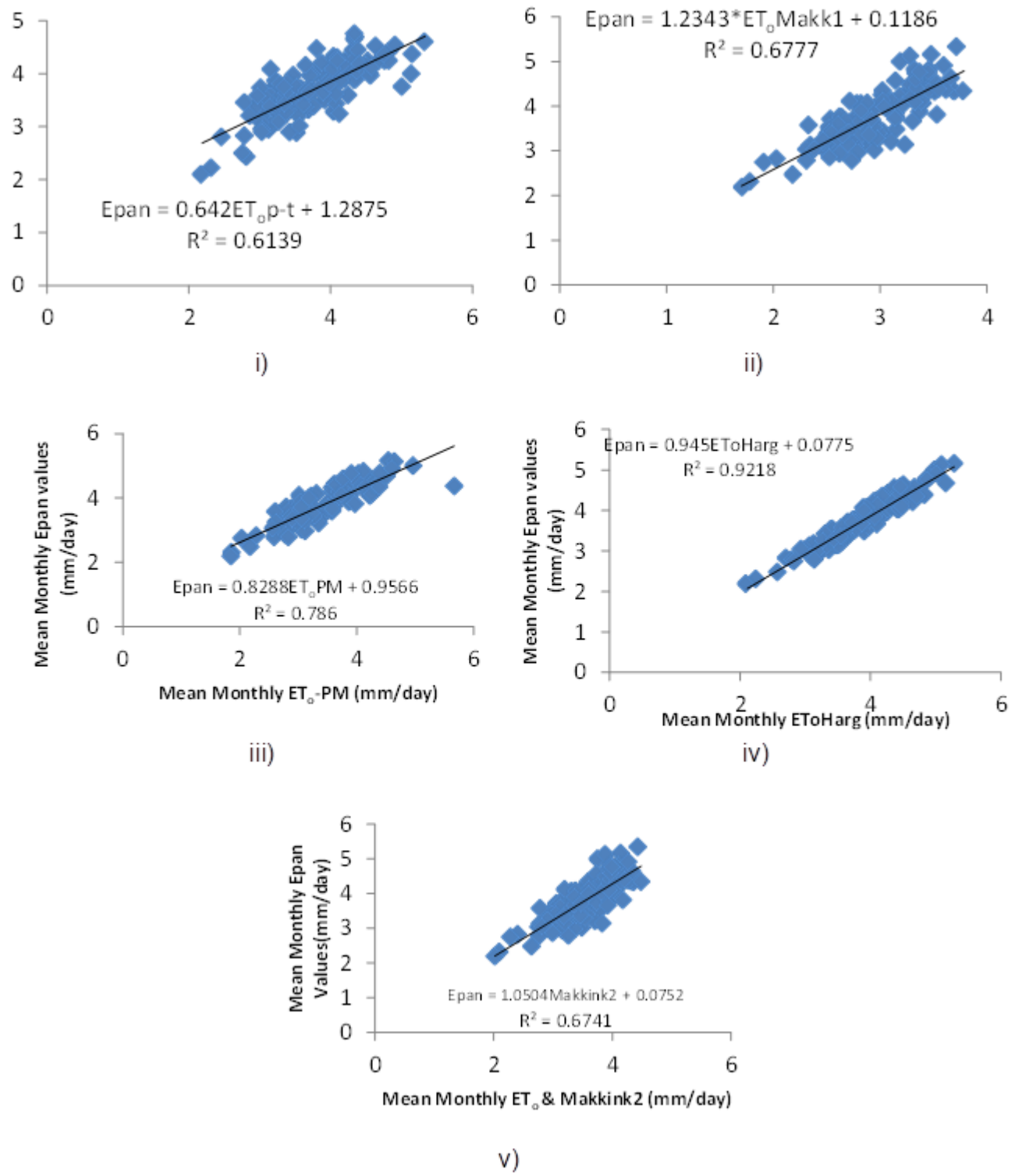

Figure 4. Regression of mean monthly Epan data against mean monthly ET_o models i) Epan versus ET_o-PT (Priestley-Taylor) ii) Epan versus Makkink-1 iii) Epan versus ET_o -PM iv) Epan versus Hargreaves-Samani and v) Epan versus Makkink-2.

regression equation of slope (b) of 1, an intercept (c) close to zero (0) and coefficient of determination (R^2) of 1, produces a perfect fit. Figures 4 and 5 show typical mean monthly plots of ET_o-PM against mean monthly ET_o values and mean monthly Epan values against mean monthly ET_o values, respectively.

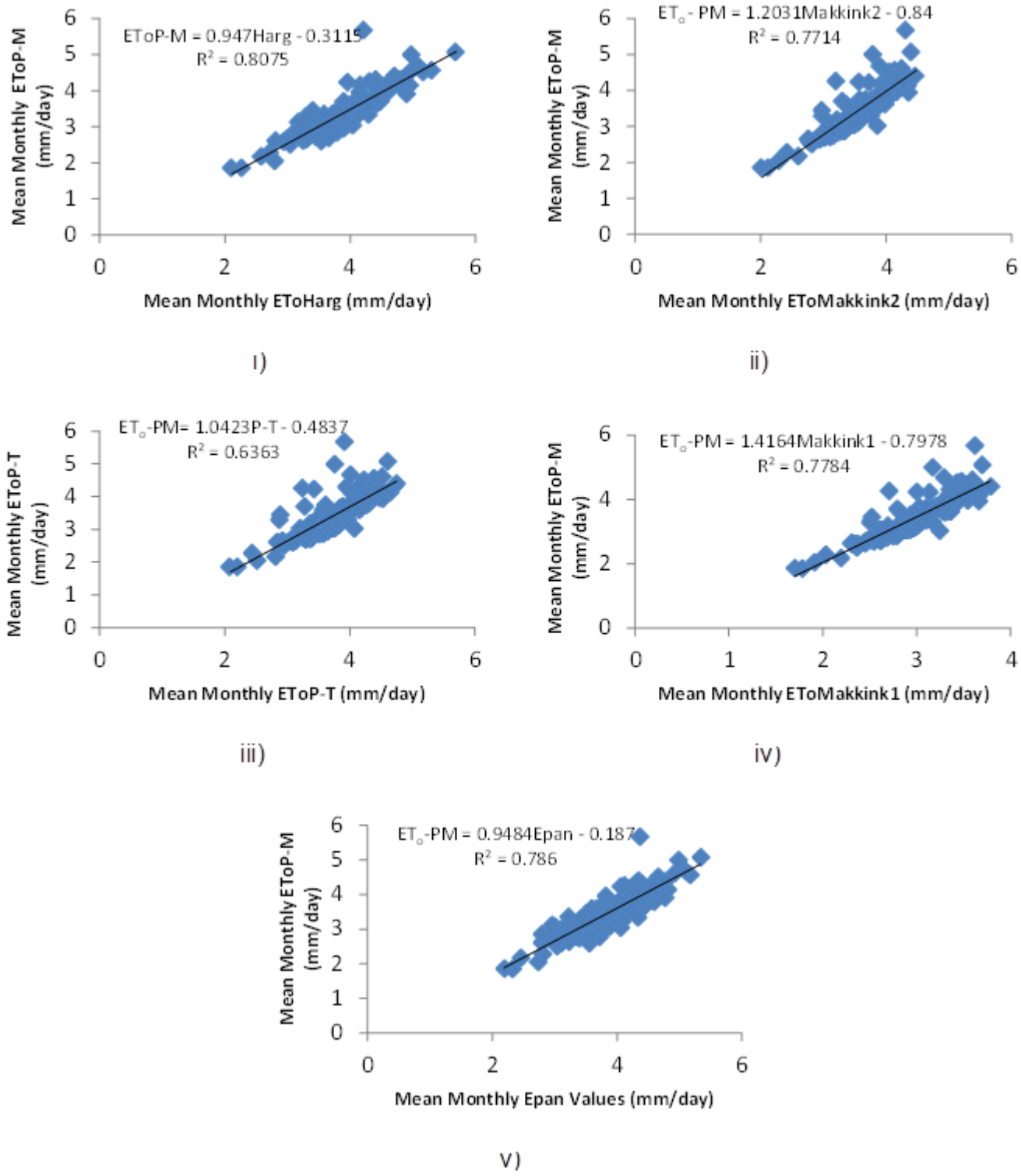

Figure 5. Regression of mean monthly ET_O - PM against mean monthly ET_o models i) ET_o - PM versus Hargreaves-Samani ii) ET_o - PM versus Makkink 2 iii) ET_o - PM versus PT (Priestley-Taylor) iv) ET_o - PM versus Makkink 1 and v) ET_o - PM versus Epan.

The cumulative ranked values of goodness of fit, R^2, slope, b and intercept, c for the regression models (Figures 4 and 5) of daily and monthly ET_o against ET_o-PM or Epan values are shown in Figures 6 and 7 and Tables A1 and A2, respectively. The correlation of daily ET_o values showed the following order of "best fit" (Figure 6):

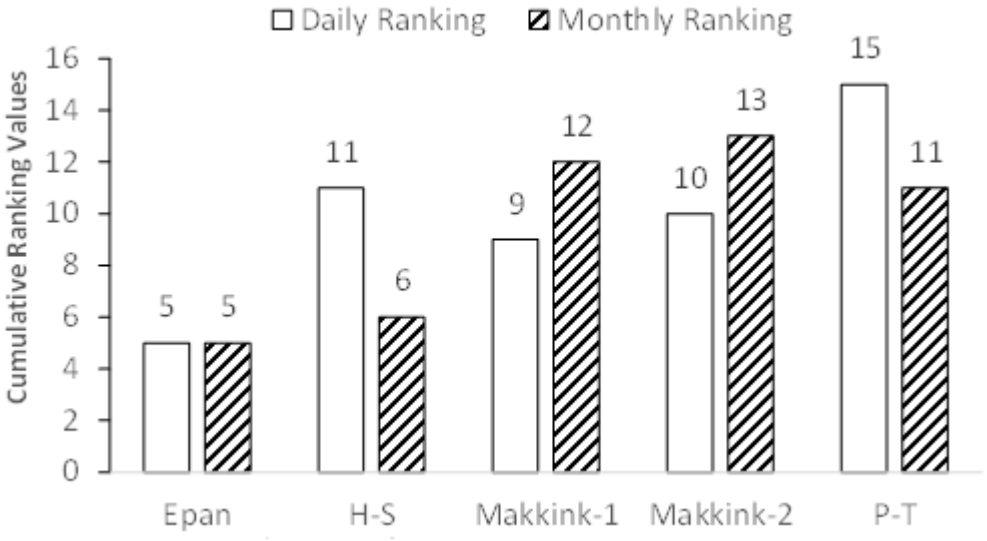

Figure 6. Comparison of best fit regression models of daily and monthly ET_o against ET_o-PM values.

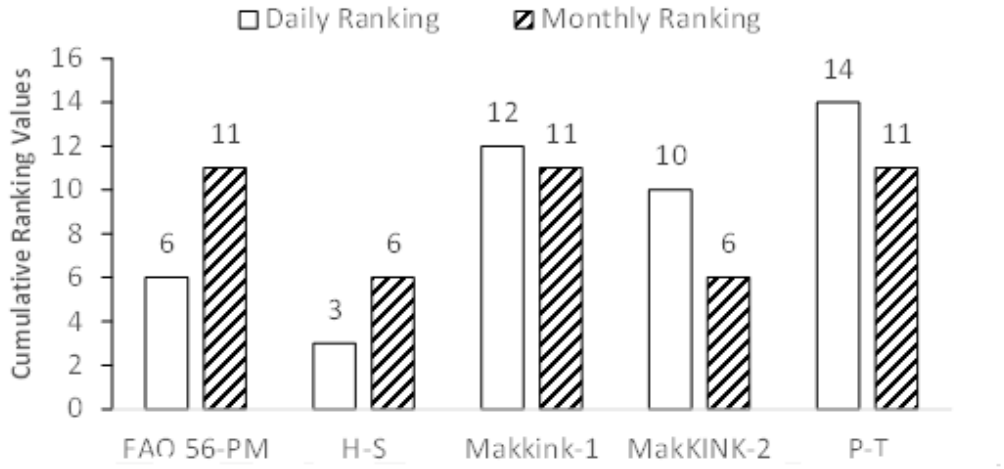

Figure 7. Comparison of best fit regression models of daily and monthly ET_o against Epan values.

1st Epan, 2nd Makkink-1, 3rd Makkink-2, 4th Hargreaves-Samani, 5th Priestly-Taylor, respectively. For the monthly ET_o against ET_o-PM linear regression models, we have: 1st Epan, 2nd Hargreaves-Samani, 3rd Priestly-Taylor, 4th Makkink-1 and 5th Makkink-2, respectively. Figure 7 shows the distribution of "best fit" regression models of daily and monthly ET_o against Epan values with respect of cumulative ranking of R^2, b and c values. For daily ET_o against Epan, the order of best fit are: 1st Hargreaves-Samani and Makkink-2, 2nd FAO 56-PM and Makkink-1, and 3rd Priestly-Taylor, respectively.

The distribution of the goodness of fit, R^2 as bench mark for the various regression models are as follows: i) 0.281 - 0.519 for daily ET_o versus ET_o-PM; ii) 0.299 – 0.836 for daily ET_o versus Epan values; iii) 0.613 – 0.922 for monthly ET_o versus Epan; and iv) 0.636 – 0.808 for monthly ET_o against ET_o-PM values, respectively.

Figure 9 shows the cumulative monthly ET_o totals for the farming season (December-April) during the study period (2000-2010). The cumulative monthly total estimated by Hargreaves-Samani was 7,136.19 mm, FAO 56-PM produced 6,448.5 mm, Priestly-Taylor- 6,538.23 mm, Makkink1- 5,298.43 mm; Makkink2- 6,280.9 mm and Epan- 7,124.32 mm.

In terms of absolute values of over/under estimation and percent relative error with Epan as benchmark, Hargreaves-Samani with original coefficient over estimated by 11.87mm and percent error of 0.17%

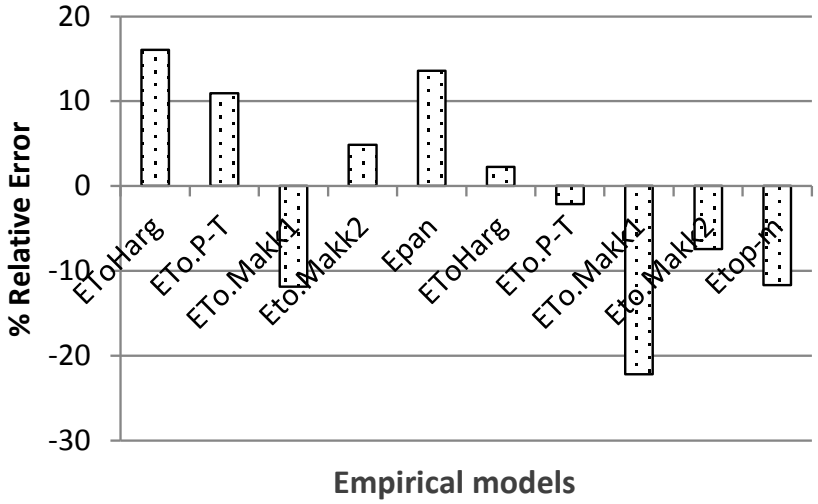

Figure 8. Percent relative error versus Epan & ET_o- PM monthly data.

ranked first, while Priestly-Taylor; 586.1 mm and 8.23%, FAO 56-PM; 675.77 mm and 9.49%, Makkink-2; 843.38 mm and 11.84% and Makkink-1; 1825.9 mm and 25.63% ranked second, third, fourth and fifth positions, respectively. With FAO 56-PM as benchmark, Priestly-Taylor ranked best by 89.68 mm and 1.39%, Makkink-2 ranked second by 167.6 mm and 2.60%, while Epan data (675.77 mm and 10.48%), Hargreaves-Samani (687.65 mm and 10.66%), Makkink-1(1,150.1 mm and 17.84%) ranked a distant third, fourth and fifth positions, respectively.

DISCUSSION

One of the objectives of this study is to find the best and approximate alternative to the standard FAO 56-PM method. The quest for the best ET_o model has prompted a global research in different climatic regions. For example, Tomar (2015) found FAO 56-PM model most appropriate for sub- humid Tarai region of Ultarakhand, India. Tabari (2010) found the Makkink model performed best in cold humid climates like the Netherlands. Amatya et al. (1995) found Turc model the best prediction method for the humid coastal plains of the United States and so on. In this study, the results of the statistical measures showed Hargreaves-Samani method ranked best for both daily and monthly evaluation with Epan data as benchmark. For the daily and monthly evaluation with FAO 56-PM as benchmark, Makkink2 (1984) ranked best while Epan data compared reasonably well with FAO 56-PM in the second position.

In terms of statistical regression analysis, Epan correlated best for daily and monthly FAO 56-PM values. Similarly, Hargreaves-Samani method correlated best with daily and monthly Epan data.

In terms of quantitative evaluation of total cumulated ET_o values for the study period (2000-2010) and cumulative monthly ET_o totals for the farming season (Dec-April) against both Epan data and FAO 56-PM, the results were in agreement with those of the statistical measures and regression analysis. Generally, Hargreaves-Samani method correlated best with Epan data, which is more evident in Figure 8 for the monthly ET_o totals for the farming season. Hargreaves-Samani scored the overall least over estimation of 11.78 mm (11 years) and percent relative error of 0.17%. With respect to FAO56-PM, both Priestly-Taylor and Makkink-2 compared best with FAO 56-PM.

The farming season is a period of high water demand and the best performance model was Hargreaves-Samani, a plausible model for the Lower Niger basin. Similar performance of the Hargreaves-Samani has been reported by Ramirez et al. (2011) for Colombian coffee zone, although in the said study, Hargreaves-Samani was evaluated against FAO 56-PM. Also Amatya et al. (1995) found Makkink and Priestly-Taylor methods in closest agreement with FAO 56-PM. The close agreement between FAO 56-PM and the radiation-based method (Makkink and Priestly-Taylor) is probably due to the prevalent low advective conditions in the Lower Niger River basin. The study agreed with Allen et al. (1998) who recommends an alternative ET_o equation to FAO Penman-Monteith equation.

The results of Equations 11 to 18 shown in Tables A1 and A2 have been used to assess the strength and weakness of the statistical measures. All the statistical measures were calculated on the basis of the relationship between observed and predicted mean deviations. The index “D” is a measure of cross-comparison between the models. Fox (1981) recommended that at least RMSE, MAE, RMSEs and RMSEu be applied in evaluating model performances and that RMSE and MAE are among the best overall measures of model performance

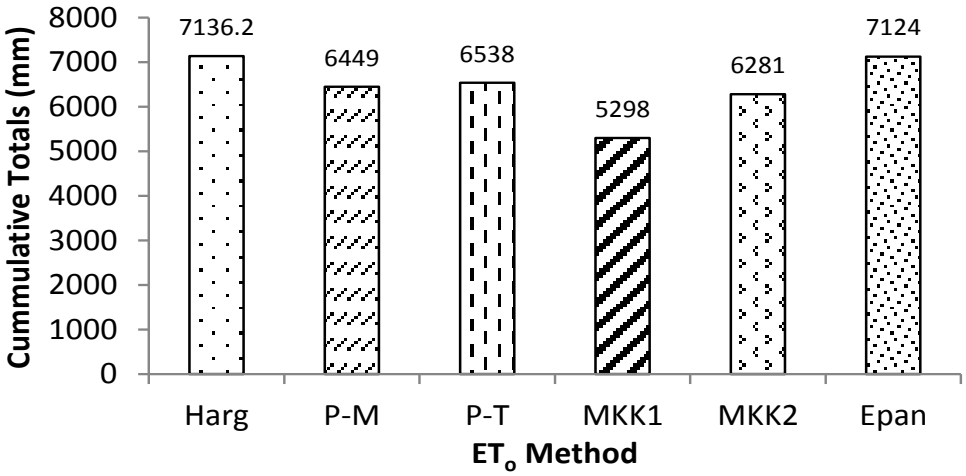

Figure 9. Cummulative totals against ET_o methods during farming season.

because they summarize the mean difference between observed(O) and predicted(P) values. The criteria adopted for assessment is that values of MAE and RMSE that are very close to zero are considered better models. According to Alexandris et al. (2008), Fox (1981) and Greenwood et al. (1985) a good model is one that has very low RMSEu and RMSEs values which are close to RMSE. From Table A1, Hargreaves–Samani has the least MBE, MAE, Sd, RMSE, RMSEs values with the exception of RMSEu, thus showing the best performance against Epan, seconded by Priestly-Taylor and thirdly by Makkink2. From Table A2, Makkink2 performed best against FAO-56 PM, seconded by Epan.

The general improvement for monthly estimates in R^2, MBE, MAE, and RMSE values indicated that the regression equations and statistical analyses for daily REF-ET values were less accurate than the monthly estimates. This greater error of prediction was due to the wide variation in daily weather parameters as compared to the mean monthly data where variability was reduced by the averaging effect.

In order to improve the accuracy of the REF-ET models against FAO 56-PM, monthly correlation factors have been computed as ratio of monthly total of PM REF-ET to the monthly total for each model as shown next.

Recalibration of model constants

From the evaluation of ET_o models against Epan data as benchmark, only Hargreaves-Samani and Priestly-Taylor methods over estimated/under estimated with a small margin of 313.4 mm and 452.3 mm in 11 years (2000-2010). With FAO 56-PM as a bench mark, only Makkink-2 (1984) method over estimated with a small margin of 512.4 mm, the other empirical models produced large margins. The existence of large margins support the need to adjust the models in a calibration process. The adjustment was achieved with the use of mean monthly correction factors. The mean monthly correction factors for ET_o models were computed as the ratio of the monthly total of FAO 56-PM to the monthly total for each method averaged over the record period (Amatya et al., 1995). Table 4 contains the estimated monthly correction factors for adjusting the ET_o models against FAO 56-PM. These adjustment factors can be used for prediction of RET- ET beyond year 2010.

Conclusion

The following conclusions were drawn from the results of the study:

i) Based on the statistical analyses, regression analysis, accumulated REF-ET values (2000 to 2010); monthly REF-ET estimates (summed daily values) for the farming season (Dec to April). Hargreaves-Samani method was in best agreement with daily and monthly Epan data. Furthermore, Hargreaves-Samani method was in best agreement with Epan data during the farming season (December - April) producing a slight over estimation of 11.87 mm and percent relative error 0.17% in 11 years.

ii) The comparison of REF-EF estimates with Epan data and FAO 56-PM as benchmarks showed that Hargreaves-Samani method was in best agreement with Epan data while Priestley-Taylor ranked best against FAO 56 PM, seconded by Makkink2 (1984) and thirdly Hargreaves-Samani method. Thus, Hargreaves-Samani performed reasonably well with FAO56-PM.

iii) The mean monthly data correlates better with Epan data and FAO 56-PM than the daily data. The three best REF-ET models are in this order: Hargreaves–Samani, Priestley-Taylor and Makkink (1984) and may be

Table 4. Estimated monthly correction factor for adjusting ET_o empirical models against ET_o-PM.

ETos / Month	Harg	P – T	MKK1	MKK2	Epan
Jan.	0.9693	1.046	1.237	1.044	0.9402
Feb.	0.9004	1.061	1.314	1.107	0.8974
Mar.	0.8637	0.9715	1.236	1.042	0.8840
April	0.8986	0.9050	1.142	0.9650	0.9428
May	0.8608	0.8949	1.1363	0.9563	0.9253
Jun	0.8712	0.8331	1.048	0.8807	0.9253
July	0.8309	0.8370	1.073	0.8970	0.9412
Aug.	0.8632	0.8162	1.044	0.8747	0.9031
Sept.	0.7741	0.8330	1.086	0.9077	0.7923
Oct.	0.8031	0.8652	1.110	0.9300	0.8003
Nov.	0.8475	0.8771	1.095	0.9213	0.8245
Dec.	0.8475	0.9554	1.156	0.9741	0.8607
Average	0.8645	0.9080	1.340	0.9584	0.8834

recalibrated using the approach stated above.

iv) The FAO – 56 PM is universally accepted the "standard" method for estimating daily or monthly ETo. A major disadvantage to the application of the standardized FAO-56 PM procedure is the relatively high data demand requiring measurements of Temperature, Rel. hum., Rs, wind speed(u) and a plethora of intermediate parameters. Another problem is linked with data quality. Lastly, another serious problem is related to the cost of instrumentation for collecting the required meteorological in automated weather stations (Valiantzas, 2013; Jensen et al., 1997; Allen, 1996). The outcome of this study corroborates with Allen et al. (1998) which recommends Hargreaves-Samani as an alternative model for ETo. Hargreaves-Samani is a temperature–based model which requires only a few input parameters such as mean temperature, minimum temperature, maximum temperature and extraterrestrial radiation (Ra). Consequently, it is an economic alternative.

CONFLICT OF INTERESTS

The authors have not declared any conflict of interests.

REFERENCES

Alexandris S, Stricevic R, Petkovic S (2008). Comparative analysis of reference evapotranspiration from the surface of rainfed grass in Central Serbia, calculated by six empirical methods against the Penman-Monteith formula. Euro. Water 21/22:17-28.

Allen GR (1996). Assessing Integrity of weather data for reference evapotranspiration estimation. J. Irrigation Drainage Eng. 122(2):97-106.

Allen GR, Pereira SL, Raes D, Smith M (1998). Crop evapotranspiration: Guidelines for computing crop water requirement. Food and Agriculture Organisation (FAO) of the United Nations. Publication No. 56, Rome. 300 p.

Allen GR, Pruitt WO (1986). Rational use of the FAO Blaney – Criddle Formula. J. Irrigation Drainage Eng. 112(2):139-155.

Amatya DM, Skaggs RW, Gregory JD (1995). Comparison of Methods for Estimating REF-ET. J. Irrigation Drainage Eng. 121(6):427-435

Berengena J, Gavilan P (2005). Reference ET estimation in a highly advective semi-arid environment. J. Irrigation Drainage Eng. ASCE 131(2).

Dash SS, Khatua KK (2016). Sinuosity Dependency on Stage Discharge in Meandering Channels, Journal of Irrigation and Drainage Engineering, ASCE, ISSN 0733 – 9437:04016030-04016030- 12.

Douglas EM, Jacobs JM, Sumner DM, Ray RL (2009). A comparison of models for estimating potential evapotranspiration for Florida land cover types. J. Hydrol. Jul 15; 373(3):366-376.

Food and Agricultural Organization of the United Nations (1990). Report on the Expert Consultation on Revision of FAO methodologies for Crop Water Requirements, Land and Water Development, Division, Rome, Italy.

Fox DG (1981). Judging Air Quality Model performance : A Summary of the American Meteorological Society Workshop on Dispersion Model Performance. Bull. Am. Meteorol. Soc. 62:599-609.

Hansen S (1984). Estimating of Potential and Actual Evapotranspiration. Nordic Hydrol. 15:205-212.

Hargreaves GH, Samani ZA (1981). Estimating Potential Evapotranspiration. J. Irrigation Drainage Division Proc. Am. Soc. Civil Eng. ASCE 108(3):224-230.

Jensen ME (1974). Consumption Use of Water and Irrigation Water Requirements, Report of the Technical Committee on Irrigation Water Requirement. Irrigation and Drainage Division ASCE, New York, N.Y.

Jensen ME, Burman RD, Allen GR (1990). Evatranspiration and Irrigation Water Requirement ASCE Manual and Report on Engineering Practical , No.70, ASCE, New York N.Y.

Jensen D, Hargreaves G, Temesgen B, Allen R (1997). Computation of ETo under non-ideal conditions. J. Irrig. Drain. Eng. 123:394-400.

Makkink H (1984). tentoonstellingscatalogus. Wetering Galerie Amsterdam 16p.

Makkink GF (1957). Testing the Penman Formula by means of Lysimeters. J. Institute Water Eng. 11:277-288.

Pogen FB, Ghosh KA, Kundu P (2016). Review on Different Evapotranspiration Empirical equations. Int. J. Adv. Eng. Manag. Sci. 2(3):17-24.

Ramirez HV, Mejia A, Marin VE, Arango R (2011). Evaluation of methods for estimating the reference evapotranspiration in Colombian Coffee. Agronomia Columbiana 29(1):107-114.

Salau OA, Lawson TL (1986). Dewfall Features of a Tropical Station: the Case of Onne (Port Harcourt), Nigeria. Theor. Appl. Climatol.

Springer-Verlag Netherlands 37:233-240.
Tabari H (2010). Evaluation of Reference Crop Evapotranspiration Equations in Various Climates. Water Resour. Manag. 24:2311-2337.
Tomar AS (2015). Comparative Performance of Reference Evapotranspiration Equations at Sub-Humid Tarai Region of Ultarakhand, India. Int. J. Agric. Res. 10:65-73.
Valiantzas JD (2013). Simplified forms for the standardized FAO -56 Penman – Monteith reference evapotranspiration using limited weather data. J. Hydrol. Elservier 505(2013):13-23.
William H, Cooke III, Grala K, Wax CL (2008). A method for Estimating Pan Evaporation for Inland and Coastal Regions of the Southeastern US. Southeastern Geographer 48:149-171.
Willmott CJ (1982). Some Comments on the Evaluation of Model Performance. Bull. Am. Meteorol. Soc. 63:1039-1313.
Xu C-Y, Singh VP (2000). Evaluation and generalization of radiation-based methods for calculating evaporation. Hydrol. Process. 14(2):339-349.
Xu C-Y, Singh VP (2001). Evaluation and Generalization of Radiation-based Method for Calculating Evaporation. Hydrol. Process. J. 15:305-319.
XU C-Y, Singh VP (2002). Cross Comparison of Empirical Equations for Calculating Potential Evapotranspiration with Data from Switzerland. Water Resour. Manag. Kluwer Academic Publishers Netherland 16:197-219.
Allen RG, Smith M, Perrier A, Pereira LS (1994a). An update for the definition of reference evapotranspiration. ICID Bull. 43(2):35-92.
Allen RG, Smith M, Perrier A, Pereira LS (1994b). An update for the definition of reference evapotranspiration. ICID Bull. 43(2):1-34.
Greenwood DJ, Neteson JJ, Drayscott A (1985). Response of Potatoes to N fertilizer: dynamic model. Plant Soil 85:185-203.
Priestley CHB, Taylor RJ (1972). On the assessment of the surface heat flux and evaporation using large-scale parameters. Mon. Weather Rev. 100:81-92.

APPENDIX A

Table A1. Summary statistics of ET_o estimation methods against Epan (daily and monthly values).

Indices	FAO 56-PM R R*	Hargreaves-Samani R R*	Makkink-1 R R*	Makkink-2 R R*	Priestley-Taylor R R*
$\bar{P}$ (mm/day)	3.80(3.37) 4 (4)	4.37(3.88) 2 (2)	3.31(2.94) 5 (5)	3.93 (3.5) 3 (3)	4.2 (3.70) 1 (1)
MBE(mm/day)	0.491(-0.381) 4 (4)	0.088(0.136) 1 (2)	-0.973 (-0.81) 5 (5)	-0.348 (-0.25) 3 (3)	-0.13 (-0.054) 2 (1)
MAE(mm/day)	0.686(0.414) 4 (4)	0.230(0.18) 1 (1)	1.05 (0.81) 5 (5)	0.615 (0.349) 3 (3)	0.56 (0.310) 2 (2)
S_d^2	0.448(0.0962) 3 (2)	0.116(0.031) 1 (1)	0.463 (0.31) 5 (5)	0.448 (0.126) 2 (3)	0.49 (0.159) 4 (4)
RMSE(mm/day)	0.830(0.491) 4 (4)	0.351(0.223) 1 (2)	1.19 (0.89) 5 (5)	0.754 (0.134) 3 (1)	0.71 (0.389) 2 (3)
RMSEu(mm/day)	0.597(0.307) 5 (4)	0.321(0.18) 4 (1)	0.27(0.23) 1 (2)	0.305 (0.28) 2 (3)	0.32 (0.315) 3 (5)
RMSEs(mm/day)	0.577(0.384) 2 (4)	0.142(0.14) 1 (1)	1.16(0.85) 5 (5)	0.690 (0.33) 4 (3)	0.63 (0.228) 3 (2)
EF	0.014(0.371) 5 (5)	0.824(0.87) 2 (2)	-1.02(-1.1) 1 (1)	0.187 (0.51) 4 (4)	0.27 (0.605) 3 (3)
D	0.750(0.862) 2 (3)	0.952(0.97) 1 (1)	0.543(0.61) 5 (5)	0.631 (0.84) 3 (4)	0.63 (0.870) 4 (2)
R^2	0.443(0.7846) 2 (2)	0.836(0.922) 1 (1)	0.38(0.678) 4 (3)	0.40 (0.674) 3 (4)	0.30 (0.614) 5 (5)
b(lope)	0.636(0.8273) 2 (4)	0.867(0.945) 1 (3)	0.251(1.234) 5 (5)	0.30 (1.050) 3 (1)	0.26 (0.956) 4 (2)
C(intercept)	1.066(0.9625) 2 (5)	0.658(0.078) 1 (2)	2.234(0.119) 3 (3)	2.70 (0.075) 4 (1)	3.05 (0.216) 5 (4)
Cumulative R & R* values	39 (45)	17 (19)	49 (49)	37 (33)	38 (34)

( ) = Estimates Based on mean Monthly values, N=3575, R =Ranking Based on Daily values; R*=Ranking Based on mean monthly values.

Table A2. Summary statistics of ET_o estimation methods against ETo_{PM} (daily and monthly values).

Indices	Epan R R*	Hargreaves-Samani R R*	Makkink1 equation R R*	Makkink2 R R*	Priestley-Taylor R R*
$\bar{P}$ (mm/day)	4.28 (3.75) 3(3)	4.37 (3.88) 5(5)	3.31 (2.94) 4(4)	3.93 (3.5) 1(1)	4.2 (3.7) 2(2)
MBE(mm/day)	0.491(0.381) 4 (3)	0.579 (0.517) 5 (5)	-0.482 (-0.43) 3(4)	0.144 (0.13) 1 (1)	0.364(0.328) 2 (2)
MAE(mm/day)	0.686(0.414) 4 (2)	0.749 (0.545) 5 (5)	0.542 (0.430) 2 (3)	0.451 (0.289) 1 (1)	0.618(0.461) 3 (4)
S_d^2	0.448(0.096) 3 (2)	0.458 (0.086) 4 (1)	0.364 (0.128) 2 (4)	0.343 (0.111) 1 (3)	0.461(0.161) 5 (5)
RMSE(mm/day)	0.830(0.491) 4 (2)	0.890 (0.594) 5 (5)	0.772 (0.555) 3 (4)	0.603 (0.356) 1 (1)	0.770(0.517) 2 (3)
RMSEu(mm/day)	0.624(0.287) 5 (4)	0.610 (0.276) 4 (3)	0.234 (0.194) 1 (1)	0.269 (0.231) 2 (2)	0.334(0.306) 3 (5)
RMSEs(mm/day)	0.545(0.398) 2 (3)	0.652 (0.530) 3 (5)	0.736 (0.520) 5 (4)	0.540 (0.271) 1 (1)	0.70(0.417) 4 (2)
EF	-0.079 (0.45)3 (2)	-0.241 (0.195) 2 (5)	0.067 (0.297) 5 (4)	0.432 (0.711) 1 (1)	0.071(0.391) 4 (2)
D	0.747(0.864) 1 (2)	0.710 (0.822) 3 (3)	0.627 (0.773) 4 (5)	0.722 (0.901) 2 (1)	0.582(0.814) 4 (5)
R^2	0.442(0.785) 3 (2)	0.410 (0.808) 4 (1)	0.519 (0.778) 2 (3)	0.519 (0.771) 3 (4)	0.28(0.636) 5 (5)
b(lope)	0.696(0.948) 1 (2)	0.634 (0.947) 2 (3)	0.305 (1.416) 4 (5)	0.350 (1.203) 3 (4)	0.261(1.042) 5 (1)
C(intercept)	1.64(-0.188) 1 (1)	1.97 (-0.312) 5 (2)	2.15 (-0.798) 3 (4)	2.61 (-0.84) 4 (5)	3.17(-0.484) 5 (3)
Cumulative R & R* Values	34 (27)	44 (43)	38 (45)	21 (22)	44 (40)

( ) = Estimates based on mean monthly values, N=132, R =Ranking based on daily values; R*=Ranking based on mean monthly values.

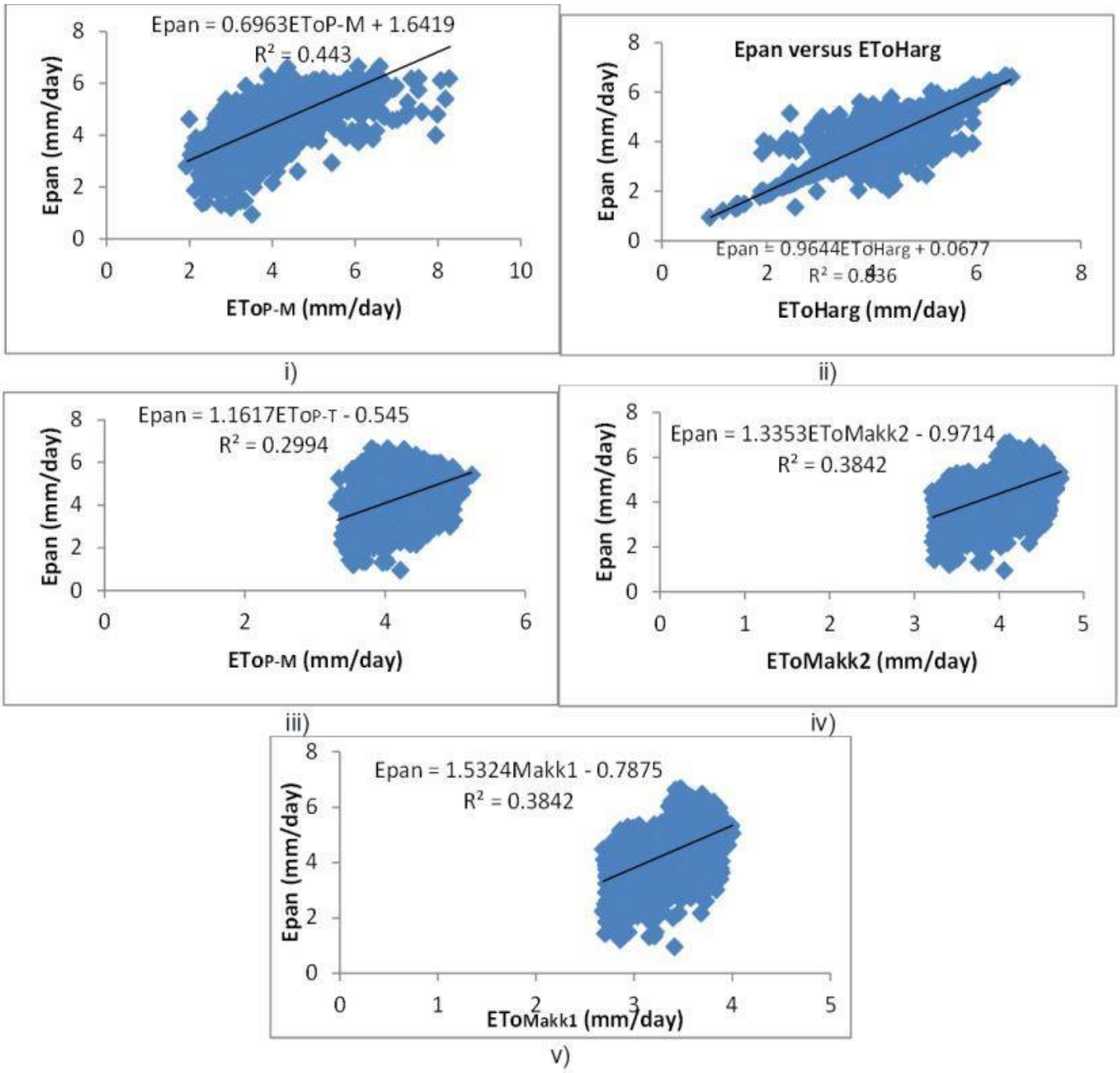

Figure 1a. Regression of Mean Monthly Epan Data against Mean Monthly ET_o models i) Epan versus ET_o PT(Priestley-Taylor) ii) Hargreaves-Samani iii) Epan versus ET_o -PM iv) Epan versus Makkink 2 and v) Epan versus Makkink 1.

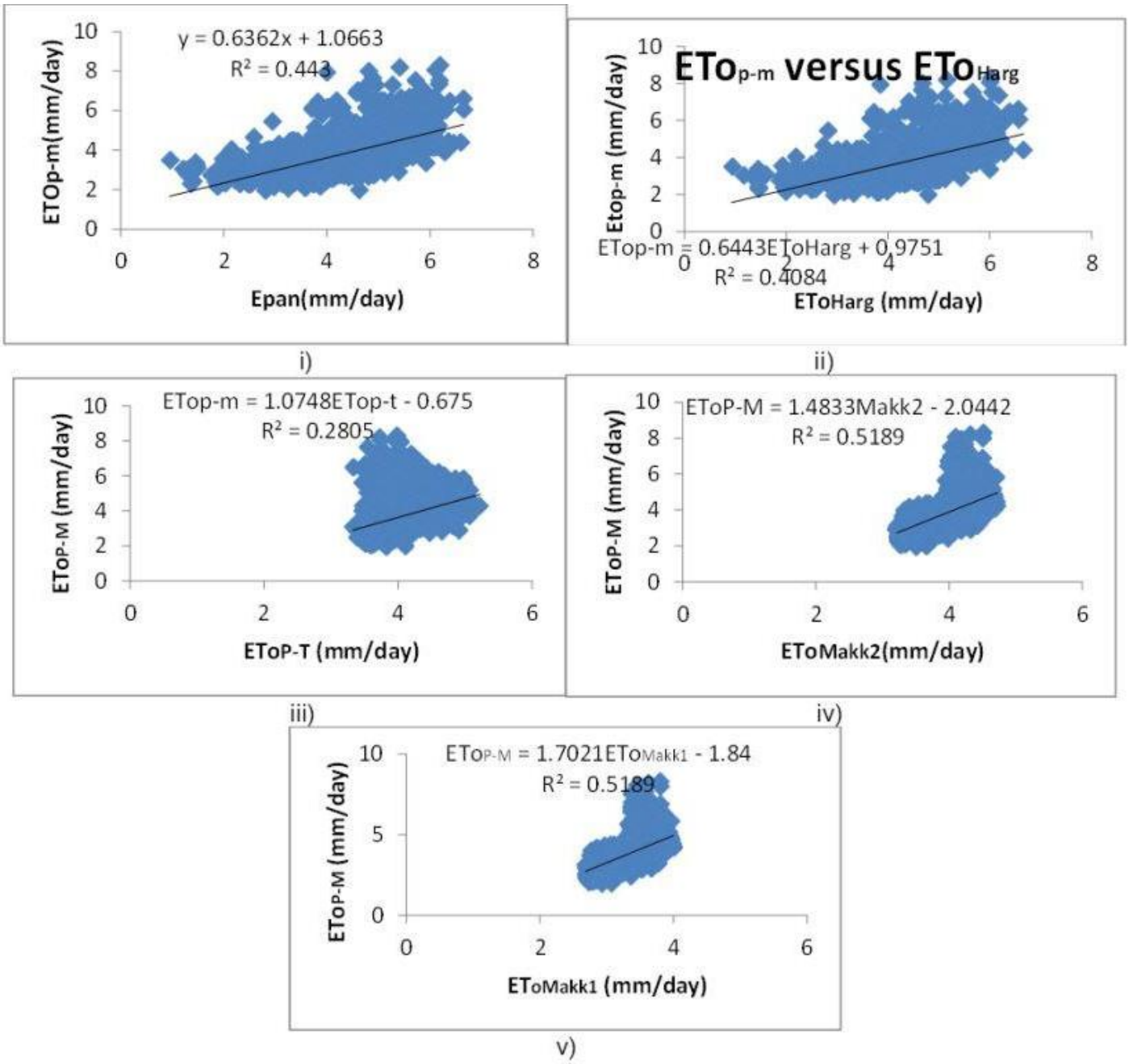

Figure 1b. Regression of Mean Monthly ET_O - PM against Mean Monthly ET_o models i) ET_o - PM versus Epan ii) ET_o - PM versus Hargreaves-Samani iii) ET_o - PM versus PT (Priestley-Taylor) iv) ET_o - PM versus Makkink 2 and v) ET_o - PM versus Makkink 1.

academicJournals

Vol. 9(8), pp. 178-190, August 2017
DOI: 10.5897/IJWREE2017.0723
Article Number: E23790265327
ISSN 2141-6613

http://www.academicjournals.org/IJWREE

International Journal of Water Resources and Environmental Engineering

Full Length Research Paper

Analysis of spatial and temporal drought variability in a tropical river basin using Palmer Drought Severity Index (PDSI)

Raphael M. Wambua[1]*, Benedict M. Mutua[1] and James M. Raude[2]

[1]Department of Agricultural Engineering, Egerton University, Kenya.
[2]Jomo Kenyatta University of Agriculture and Technology, SWEED, Kenya.

Received 24 April, 2017; Accepted 14 June, 2017

Analysis of spatial and temporal drought variability in the upper Tana River basin using Palmer Drought Severity Index (PDSI) was conducted. The drought is critical for formulation of mitigation measures in the river basin. A monthly temporal and 90-m spatial resolution was applied. This was achieved within ArcGIS environment. Climatic data for 1970 to 2010 was used for computation of the PDSI while the missing data sets were filled using Artificial Neural Networks (ANNs). The results of PDSI for dry and wet seasons at meteorological stations indicate that the time series plots for the PDSI values for dry season are generally lower than those for the wet seasons. The PDSI values for meteorological stations located at the lower elevation of the basin are lower than those located at higher elevation. On the other hand, spatially distributed drought severity based on PDSI show that the ranges of maximum and minimum drought severity values in 1970 are -0.868 to -0.804 and -0.675 to -0.610 respectively. These values of drought severity occur respectively in the north-western and south-eastern areas of the basin. PDSI values increased from the range -0.675 to -0.610 in 1970 and from -1.087 to 0.957 in 2010 for the north-eastern areas of the upper basin. The south eastern areas of the basin are more prone to drought risks than north-western parts. Use of the PDSI reflects the spatial heterogeneity and temporal variability of drought across the basin. The drought assessment offer technical approach for comprehensive understanding of drought for effective drought-induced disaster mitigation and its management, with a view to reducing adverse effects on livelihoods.

Key words: Palmer Drought Severity Index (PDSI), drought severity, upper Tana River basin, monthly resolution, drought-induced disaster.

INTRODUCTION

Drought is a condition on land characterised by scarcity of water that falls below a defined threshold level. The term drought has been defined differently in numerous applications (UNDP, 2012). However, it is a challenge to quantitatively define the term. Droughts may be expressed in terms of indices that depend on

*Corresponding author. E-mail: wambuarm@gmail.com.

precipitation deficit, soil-water deficit, low stream flow, low reservoir levels and low groundwater level. Drought may be defined differently depending on the sector involved. For example, a hydrological-drought occurs whenever river or groundwater levels are relatively low. In addition, water-resources drought occurs when basins experience low stream flow, reduced water reservoir volume and groundwater levels. The water resources drought is influenced by climatic and hydrological parameters within a river basin and drought management practices. The hydrological drought, mainly deals with low stream flows. This drought adversely affects various aspects of human interest such as food security, water supply and hydropower generation (Karamouz et al., 2009; Belayneh and Adamowski, 2013).

It is paramount to analyse and monitor drought due to its adverse effects. For the purpose of understanding drought, the hydro-meteorological variables are encapsulated into drought indices at river basin scales. These drought indices provide critical information on decision making (Quiring and Papakryiakou, 2003). In order to mitigate adverse drought impacts on water resources, ecosystems, economy and peoples livelihoods, it is paramount to undertake drought studies. Key drought studies should describe its characteristics such as temporal trends, spatial distribution of severity frequency and duration. Prior to formulation of drought mitigation mechanism in a river basin, it is essential to first describe its characteristics at the basin scale. Drought affects ecosystem response mechanisms and is thus perceived to influence the future of the global earth carbon balance (Bonal et al., 2016).

In this study, upper Tana River basin was selected because it is a very important resource in Kenya. It is clipped from the larger Tana River basin; the largest river basin in the country that provide huge water resources. The upper Tana River basin has forest land resources located along the eastern slopes of Mount Kenya and Aberdares range which have a critical role in regulating the hydrology of the entire basin (IFAD, 2012). The basin is located within a fragile ecosystem that represents all agro-ecological zones of Kenya where water resource systems, hydro- power generation and food security are negatively impacted by frequent drought occurrences.

A number of drought types have been recognized by previous researchers. According to Zoljoodi and Didevarasl (2013), there are four main categories of droughts; Hydrological, Meteorological, Agricultural and Socio-economic droughts. The first three types are called the operational droughts and can be integrated into a drought management process. Their relation can be used in development of water resources program within a river basin (Karamouz et al., 2003). Propagation of hydrological and agricultural drought starts from meteorological droughts induced by changing phenomena within the hydrological cycle (Figure 1).

The three operational types of droughts are interconnected. For instance, Agricultural drought links meteorological and/or hydrological drought to agricultural impact. Agricultural droughts impact negatively on farming systems whenever they occur. Their impacts are normally two-fold; environmental and economic impacts. The agricultural drought is a type associated with low agricultural production, increased food insecurity, decline in output from agro-processing industries and unemployment incidents in the agricultural sector. From the environmental perspective, agricultural drought is caused by insufficient precipitation, high temperature that causes elevated rates of evapo-transpiration, increased salt concentration in the crop root zones and soils within irrigation systems (Mishra and Singh, 2010). The term environmental drought is sometimes used to address the adverse effects of extremely low flows on ecosystems, and may be analysed in the emerging field of eco-hydrology.

Based on purpose for research, drought indices have previously been developed and applied on drought studies. Some of the most common drought indices include palmer drought severity index (PDSI), standardized precipitation index (SPI), surface water supply index (SWSI), soil moisture deficit index (SMDI), vegetative index (VI) and stream flow drought index (SDI). In the present study, PDSI was used to analyse drought episodes in the uppar Tana River basin.

Several coefficients which are calculated to define local hydrological characteristics influenced by precipitation and temperature are calculated for use in PDSI. These coefficients depend on soil water capacity of the principal layers. The PDSI has been applied on a number of catchments for detecting and planning of drought relief programmes (Loucks and Van Beek, 2005). In the present study, spatial and temporal drought variability in the upper Tana River basin was analysed using Palmer Drought Severity Index (PDSI) to detect the drought prone areas and the severity drought events for the period 1970 to 2010.

MATERIALS AND METHODS

Study area

The study area; upper Tana River basin is located within latitudes 00° 05' and 01° 30' south and longitudes 36° 20' and 37° 60' east. The study area covers 17,420 km^2 and is illustrated in Figure 2).

Upper Tana River basin is a portion of the Kenya's largest rivers system called Tana River basin (Jacobs et al., 2004; WRMA, 2010). There are very important vast land and forests on eastern slopes of Mount Kenya and Aberdares range within the study area. The river basin greatly regulates the hydrological processes (IFAD, 2012) and as subsequently influence the hydro-electric generation. This basin is plays a key role in hydro-electric generation, water supply and agricultural production in Kenya.

Climatic data acquisition

The data, precipitation, potential, soil moisture content and

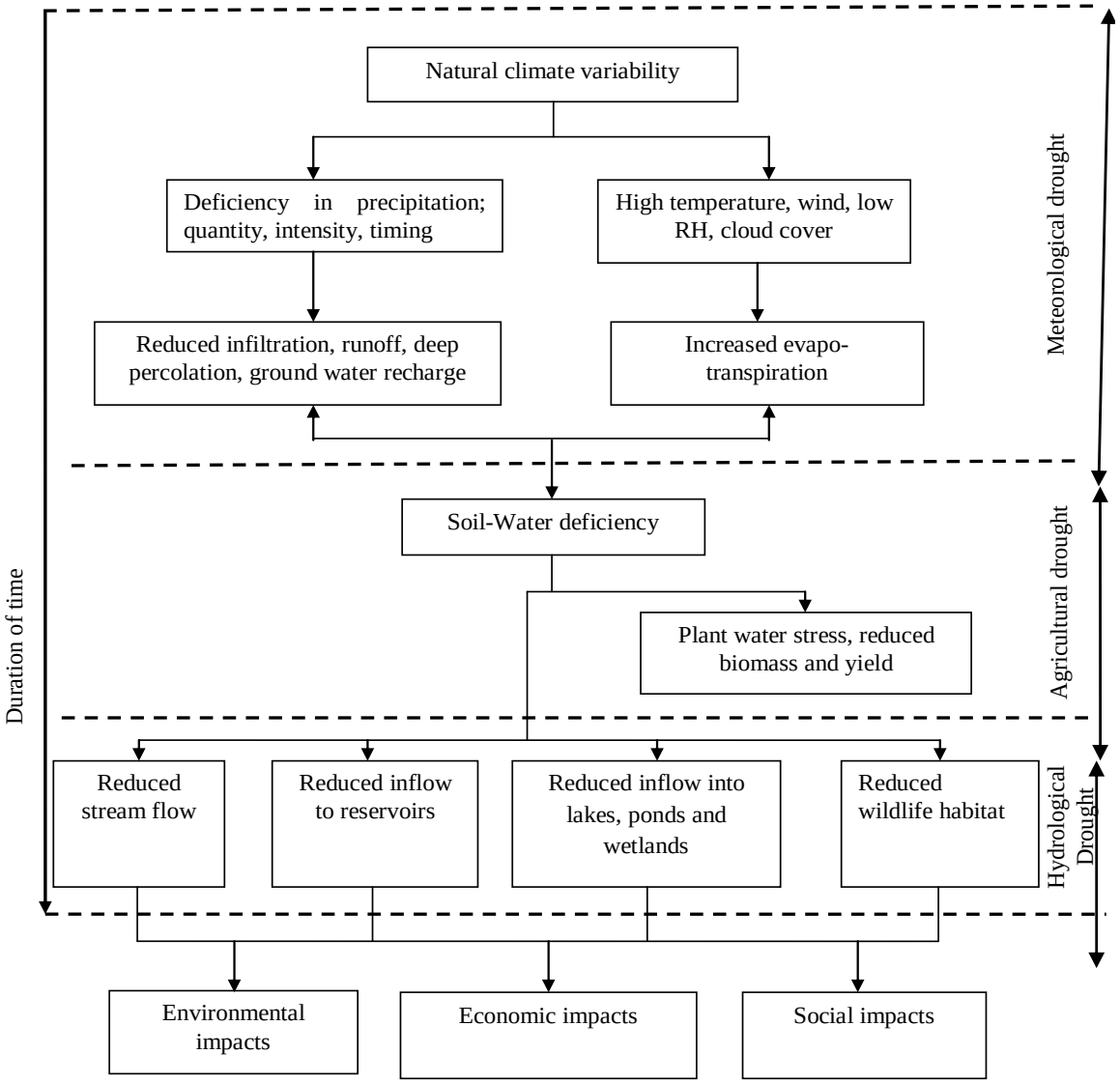

Figure 1. Propagation of drought via hydrological cycle.

temperature were used in computation and analysis Palmer Drought Severity Index (PDSI). The climatic data ranged from 1970-2010 (41 years) were used in this study. Part of this data was available while the missing data was estimated for all variables. The available data was on daily time step but had to be re-organized into monthly average time scales for all the variables to match with the data requirements of the present research. The daily stream and monthly flow data was obtained from the Ministry of Environment and Natural Resources, and Water Resources and Management Authority (WRMA).

In the upper Tana River basin, data from twenty four meteorological stations were obtained from the Ministry of Water and Irrigation. The stations provided meteorological; precipitation, temperature, evaporation data. The data were then subjected to exploratory data processing. It was found out that only eight stations had reliable and sufficient data. Where the available data contained less than 20% data gaps, then these data were selected for computation of the PDSI. The eight stations used in the study (Table 1) were also objectively located within the low (LE), lower middle (LME), middle (ME) and high (HE) elevations. The stations are located at different agro-ecological zones of the basin.

Consistency test of the climatic data

A double-mass curve was fitted for the collected hydro-meteorological data to test for consistency. The homogeinity of climatic data time series data was conducted to detect for any possible errors resulting from the data measurements. In addition, homogeneity was used to check for the fluctuations due to climate changes. The cumulative total climatic variable, precipitation were computed for each station and then plotted against the cumulative total of an adjacent station (Figure 3). Any sudden change in the gradient of the double-mass curve was considered to indicate inconsistency in the data. Although there were some changes at some points on the curves for some stations, it was considered insignificant for the present study.

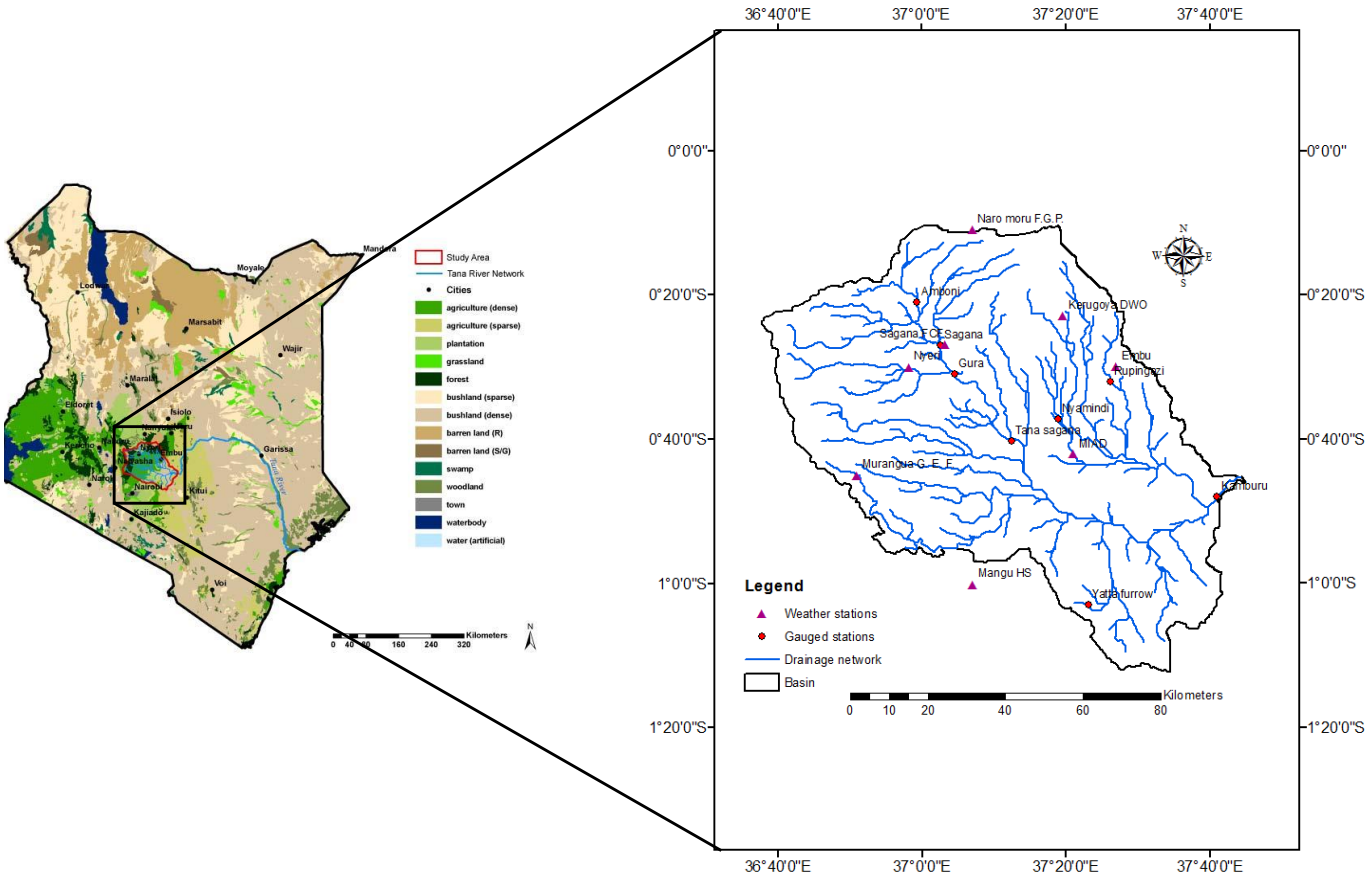

Figure 2. The location of the upper Tana River basin in Kenya.

Table 1. Meteorological stations.

S/No.	Station name	Station ID	Coordinates		Elevation (m)
			Longitude (Degrees)	Latitude (Degrees)	
1	MIAD	9037112	37.350	-0.700	1246
2	Embu	9037202	37.450	-0.500	1494
3	Kerugoya DWO	9037031	37.327	-0.382	1598
4	Sagana FCF	9037096	37.054	-0.448	1234
5	Nyeri	9036288	36.970	-0.500	1780
6	Maragua G. E. F.	9036212	36.850	-0.750	2296
7	Naro-Moru F.G.P.	9037064	37.117	-0.183	2296
8	Mangu HS	9137123	37.033	-1.100	1630

Filling in missing data

The meteorological stations; 9037064, 9037112, 9037031, 9137123, 9037202, 9037096, 9036288 and 9036212 (Table 2) had continuous data for 26, 28, 35, 32, 40, 35, 40 and 23 years respectively. The data for each station was partitioned into training and validation data sets comprising 70% and 30% respectively of the total continuously recorded data.

In this study, the ANN structure for each station was obtained by considering different input neurons for different time delays; *t, t-1, t-2,…, t-n*, in the input layer. The number of input variables was equal to the input neurons. The initial number of hidden neurons of the ANN model architecture was determined using the procedure adapted from Belayneh and Adamowski (2012) where the hidden layer neurons were initially set at $2n+1$ where n is the input neurons. The Hidden Neurons (HN) were then increased and decreased through trial and error technique for data sets at each hydrometric station. This resulted to an output that was taken as the estimated variable.

The output layer comprises neurons in all the networks that are equal to the following month's variable value (I_{t+1}). In this study, the

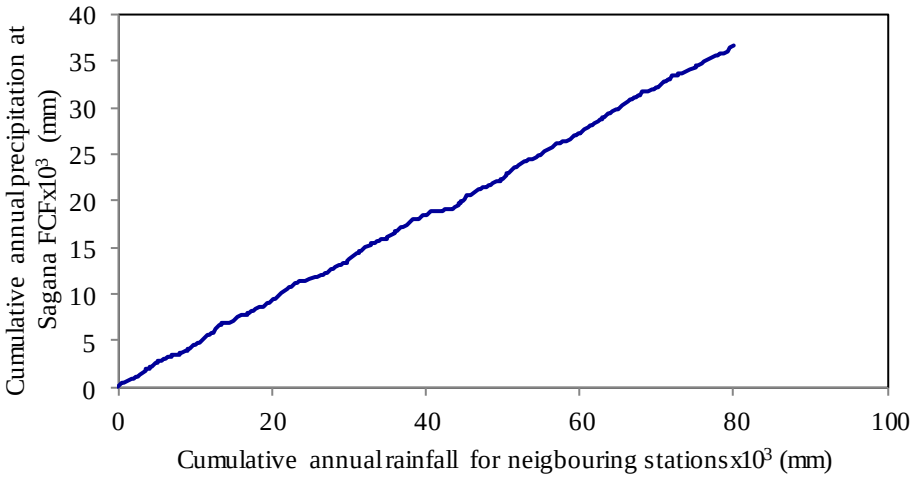

Figure 3. Double mass curve based on precipitation upper Tana River basin.

Table 2. Dominant soils for the upper Tana River basin.

Elevation	Dominant soil type	MC at saturation %	MC at field capacity %	MC at wilting point %	AWC (%)	TAW (mm)
HE	Andosols	60	40	24	16	172
ME	Nitosols	53	31	22	9	98
LME	Cambisols	48	28	14	14	74
LE	Ferralsols	53	26	17	9	82

HE, ME, LME, LE means highest elevation, middle elevation, lower middle elevation and lowest elevation respectively. Source: Hunink et al. (2009).

Feed Forward Neural Network (FFNN) and Recursive Neural Network (RNN) were applied and tested in the model training. Initially three different training algorithms were applied to train the structures. These were the back-propagation (BP), Levernberg-Marquardt (LM) and Conjugate Gradient (CG) algorithms. From preliminary results, it showed that a three-layer feed forward neural network with different input and hidden neurons was superior in performance, and that the best results were also obtained using the LM training algorithm. Thus the best ANN structure of three-layer feed forward network based on LM training algorithm was adopted for filling in of missing data in this study. The data was first normalized at each station before exporting it into the graphical user interface (GUI) of the MATLAB. This was done by applying the function given in Equation (1) which was adapted from Morid et al. (2007).

$$X_n = X_{\min} + \frac{(X_o - x_{\min})}{(x_{\max} - x_{\min})} \times (X_{\max} - X_{\min}) \quad (1)$$

Where,
X_n = normalized value
X_{min} = the selected minimum value for standardization
X_{max} = the selected maximum value for standardization
X_o = original value
x_{min} = minimum value present in the original data set
x_{max} = maximum value present in the original data set.

All the input and output values for ANN were normalized to range between X_{min} of equal to 0.1 and X_{max} of less than 1. According to Morid et al. (2007), the values of the X_{min} 0.1 and X_{max} of 0.9 perform best for drought indices such as SPI and EDI. Thus these values were adapted for this study. After normalization, the various drought forecasting ranges were determined.

For each of the ANN model run on the graphical user interface (GUI) of the MATLAB performance was evaluated based on the correlation coefficient *R* and Mean Square Error (MSE) criteria and the best model. The best ANN models were then adopted for filling any missing data for respective hydro-meteorological stations. The steps that were followed in filling the missing data are summarized in Figure 4.

Computation of drought using PDSI

The Palmer Drought Severity Index (PDSI) was developed based on a criterion for determining the beginning and end of drought or wet period spell (Palmer, 1965; Wang, 2010). It is a simple monthly water balance model which requires rainfall, temperature and catchment soil moisture content as input parameters. This tool applies a concept of supply and demand over a two-layer model. In this concept, the difference between the quantity of precipitation needed to maintain a natural water balance level and the actual precipitation is determined. The index does not consider stream flow, reservoir water balance, and other hydro-meteorological variables that influence the drought (Karl and Knight, 1985; Yan et al., 2013a; b). The index has been modified and applied by a number of researchers. For instance Wondie and Terefe (2016) used a self-calibrated PDSI to assess drought in Ethiopia for the period 1901 to 2014).

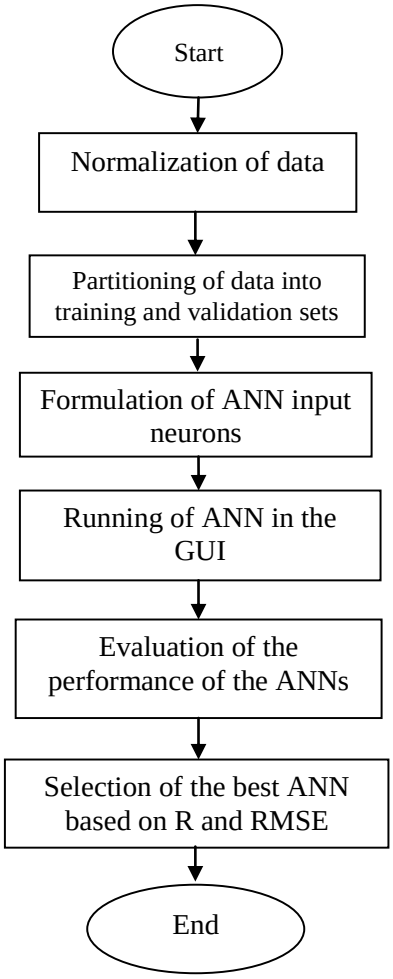

Figure 4. Flow chart of the steps used in filling the missing data using ANN.

The Palmer Drought Severity Index (PDSI) was computed using precipitation, temperature and the local Available Water Content (AWC) of the soil as the input variables. The available water capacity (AWC) and Total Available Water (TAW) were estimated based on the dominant soil characteristics for the each elevation band of the upper Tana River basin. For the gauge stations within the four partitions of elevation bands, the AWC values adapted for PDSI computation were 172, 98, 74 and 82 mm which were based on values given in Table 2, for defined dominant soil types. Table 3 shows some of the physical and chemical properties of the dominant soils.

The PDSI was determined by getting the difference between actual precipitation and water deficiency or surplus in any given month *i*. This was achieved by applying the relation:

$$d_i = P_i - \hat{P}_i \quad (2)$$

Where, d_i = difference between actual precipitation and p_i and the climatically appropriate for existing conditions (mm)
P_i = actual precipitation (mm)
$\hat{P}_i$ = an indicator of water deficiency or surplus in month *i.*

The water deficiency or surplus was estimated from the relation:

$$\hat{P} = \alpha PE_i + \beta PR_i + \gamma PRO_i + \delta PL_i \quad (3)$$

Where, $\hat{P}_i$ = an indicator of water deficiency or surplus in month *i* (mm).
PE_i = potential evapo-transpiration of month *i* (mm).
PR_i = potential recharge that gives the quantity of water required to bring the soil to its water holding capacity (mm).
PRO_i = the potential runoff (which is defined as the difference between the precipitation and potential recharge (mm).
PL_i = potential loss or the amount of soil moisture that could be lost from soil by evapo-transpiration during a zero precipitation period (mm).

The potential evapotranspiration was estimated using Hargreaves method adapted from Sivaprakasam et al. (2011) given as:

$$PE = 0.0023 \times R_a \times (T_{mean} + 17.78) \times (T_{\max} - T_{\min})^{0.5} \quad (4)$$

Where, *PE* = potential evapotranspiration (mm/month).
R_a = solar/extra-terrestrial radiation (MJ m^{-2} $month^{-1}$).
T_{mean} = mean monthly temperature (°C).
T_{max} = maximum monthly air-temperauture (°C).
T_{min} = minimum monthly air-temperature (°C).

The *α, β, γ* and *δ* are climatic coefficients which provide mean value averaged within the base period. These coefficients were computed from the following relations:

$$\alpha = \frac{\overline{ET}}{\overline{PE}}\ ,\ \beta = \frac{\overline{R}}{\overline{PR}}\ ,\ \gamma = \frac{\overline{RO}}{\overline{PRO}} \text{ and } \delta = \frac{\overline{L}}{\overline{PL}} \quad (5)$$

Where, $\overline{ET}$ = mean actual evapo-transpiration (mm).
$\overline{PE}$ = mean potential evapo-transpiration (mm).
$\overline{R}$ = mean actual recharge (mm).
$\overline{PR}$ = mean potential recharge (mm).
$\overline{RO}$ = mean actual runoff (mm).
$\overline{PRO}$ = mean potential runoff (mm).
$\overline{L}$ = mean water loss due to evapo-transpiration when precipitation is zero (mm).
$\overline{PL}$ = mean potential water loss (mm).

The values of monthly PR_i, PRO_i and PL_i were derived from the generated results of soil water content for every month *i* using the technique given by Yan et al. (2013a; b). These variables were calculated from the following relations:

$$PR_i = AWC - SW_{i-1} \quad (6)$$

$$PRO_i = SW_{i-1} = AWC - PR_i \quad (7)$$

$$PL_i = \min(PE, SW_{i-1}) \quad (8)$$

The d_i was then converted into indices of moisture anomaly z_i which was calculated using the equation:

Table 3. Physical-chemical properties of the dominant soils (Muchena and Gachene, 1988).

Soil type	Particle size distribution (%)			Organic carbon content (%)	Nitrogen content (%)
	Sand	Silt	Clay		
Andosols	5	35	60	2.20	0.66
Nitosols	16	10	74	0.76	0.25
Cambisols	56	22	22	5.77	1.10
Ferralsols	35	15	49	2.3	

Table 4. Classification of drought based on PDSI.

Value of index	Drought classification
4.00 or more	Extremely wet
3.00 to 3.99	Very wet
2.00 to 2.99	Moderately wet
1.00 to 1.99	Slightly normal
-0.50 to -0.99	Incipient wet
0.49 to -0.49	Near normal
-0.50 to -0.99	Incipient drought
-1..00 to -1.99	Mild drought
-2.00 to -2.99	Moderate drought
-3.00 to -3.99	Severe drought
-4.00 or less	Extreme drought

$$z_i = k_1 \times d_i \quad (9)$$

Where, k_c = climatic characteristic that was estimated using the relation:

$$k_1 = \frac{\left(\overline{PE} + \overline{R}\right)}{\left(\overline{P} + \overline{L}\right)} \quad (10)$$

The PDSI function was used in this study is of the form:

$$PDSI_i = 0.897\ X_{i-1} + \frac{Z_i}{C_1} \quad (11)$$

Where, *PDSI* = The PDSI for the i^{th} month
X_{i-1} = previous months PDSI
Z_i = Palmer Moisture Anomaly Index (*PMAI*)

The value of PDSI for the initial month of was taken as equal to $\frac{Z_i}{C_1}$.

The Z_i (PMAI) is expressed as:

$$Z_i = \frac{C_2\ D}{\sum_1^{12} D k_2} \times d_i \quad (12)$$

Where, k_2 = weighting factor
d = water deficiency (mm)
c_2 = conceptual parameter
D = absolute value of d
In this study, a C_2 value of 438.91 adapted from Yan et al. (2013a; b) was used. The k_2 which is a function of average water demand and supply (Barua, 2010; Yan et al., 2013a; b; Zoljoodi and Didevarasl, 2013) was estimated using the relation:

$$k_2 = C_3 \log_{10}\left(\frac{\left(\overline{PE} + \overline{R} + \overline{RO}\right)}{\left(\overline{P} + \overline{L}\right)\overline{D}}\right) + C_4 \quad (13)$$

Where, $\overline{D}$ = mean of the absolute values of d

The conceptual parameters C_3 and C_4 were equated to 1.2459 and 3.3684 respectively adapted from Yan et al. (2013a; b). The computed *PDSI* values were used to classify drought conditions based on the threshold levels given in Table 4 which was adapted from Palmer (1965) and Castano (2012). The drought severity was computed for 1970 and 2010 based on the severity equation. The area for each severity class was captured using the ArCGIS and summarized in Table 5.

Computation of drought severity

Evaluation of spatial distribution of drought severity

The sum of drought severity (DI_d) values below zero during each year for the study period was calculated. The probability P of drought occurrence was determined by dividing the number of months that had *DI* values less than zero by 12 months of the year. The drought severity was then computed at each station using the relation:

$$S = \sum_{N=1}^{N} DI_d \times P \quad (14)$$

Table 5. Drought Category-Area-Distribution (CAD) as detected using PDSI for October in 1970 and 2010.

Drought category	Drought criterion	1970		2010	
		Area (km^2)	%	Area (km^2)	%
Extreme drought	-4 or less	3758.01	21.57	4540.36	26.06
Severe drought	-3 to -2.99	1784.90	10.25	2537.551	14.57
Mild drought	-2.00 to -2.99	2062.56	11.84	1675.444	9.62
Slight drought	-1.00 to -1.99	2643.58	15.18	1824.072	10.47
Normal	0.49 to -0.49	1946.48	11.17	1964.556	11.28
Slightly wet	2.00 to 2.99	1782.32	10.23	1893.08	10.87
Moderate wet	3.00 to 3.99	1681.05	9.65	1420.637	8.16
Extremely wet	4.00 or more	1761.10	10.11	1564.297	8.98

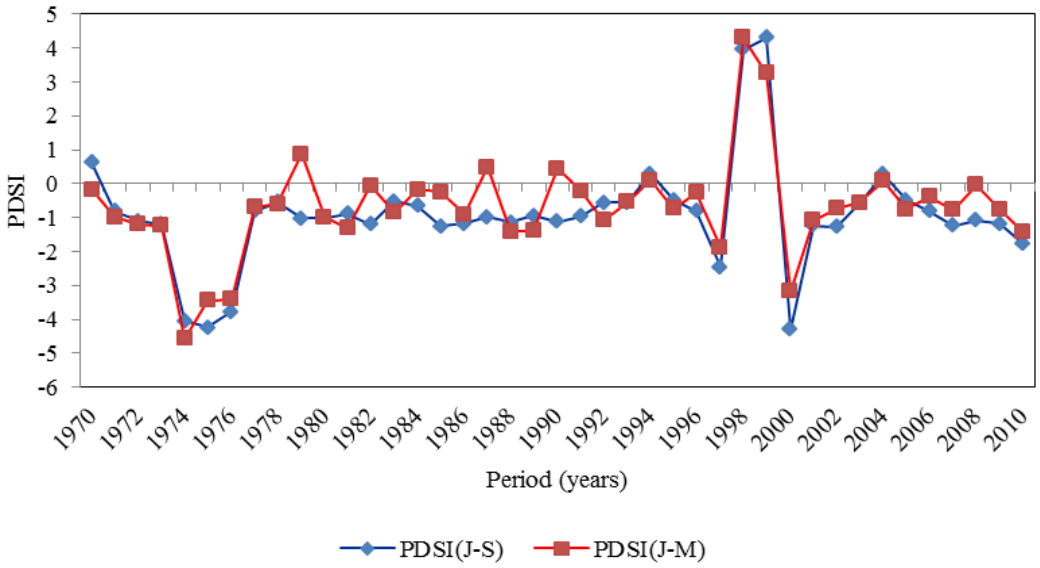

Figure 5. Time series of PDSI for dry seasons of at MIAD meteorological station.

Where, S = annual drought severity for a defined year
DI_d =The *sum* of drought severity values below zero during a particular year
P = probability of drought occurrence for the defined year
N=period in months in the year (=12 months in this case).

The resulting data was then used to estimate spatial distribution of drought severity using the Krigging estimator in the ArcGIS 10.1. In this study, sixteen hydrometric stations within the upper Tana River basin were used for hydrological evaluation. These stations have unique geographical location and their spatial extent was created through the application GIS. The GIS tool was used to compute and present the spatial distribution, variation and trends of droughts for PDSI.

RESULTS

Temporal drought patterns of the PDSI

Figures 5 and 6 illustrate the frequencies and duration of integrated seasonal droughts and wet spells as detected by the PDSI. For Figures 5 to 8, within the four decades, moderate (PDSI=-2.00 to -2.99), severe (PDSI=-3.00 to -3.99) and extreme (PDSI=-4 or less) droughts were detected using the PDSI during the dry season in the MIAD station.

For the Naro-Moru meteorological station, moderate (PDSI=-2.00 to -2.99), severe (PDSI=-3.00 to -3.99) and extreme (PDSI=-4 or less) droughts were detected during the dry season. Figures 7 and 8 that the PDSI time series values for MIAD meteorological station (ID 9037112) located at the lower elevation of the upper Tana River basin are lower than those for the Naro-Moru station (ID 9037064).

Results of the mean monthly temporal PDSI values indicate that March and April exhibit moderate (PDSI=-0.200) and extreme (PDSI=-4.00) droughts respectively. For the months of September, October and November extreme (PDSI<-4.00), incipient (PDSI=-0.5) and extreme

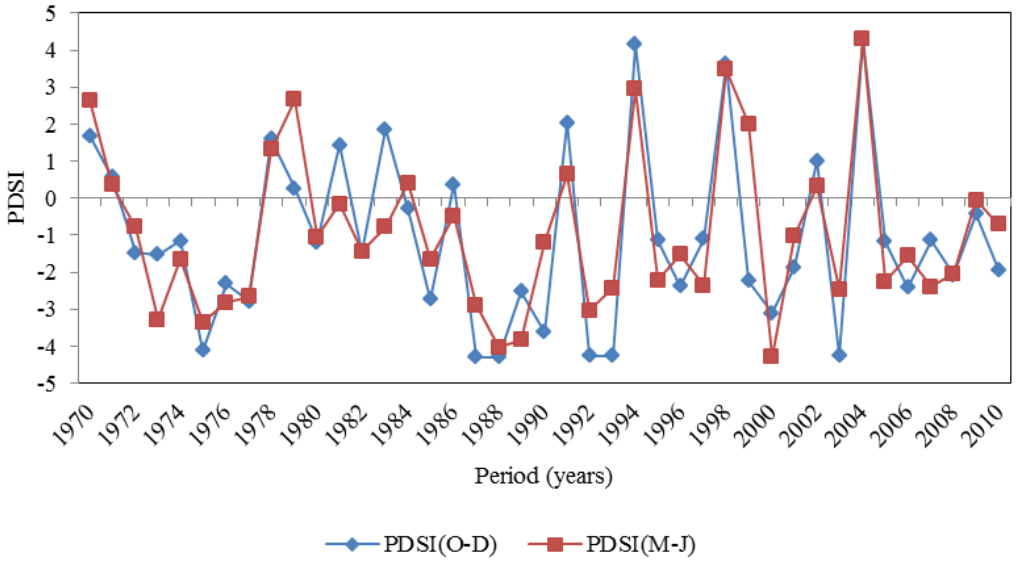

Figure 6. Time series of PDSI for wet seasons at MIAD meteorological station.

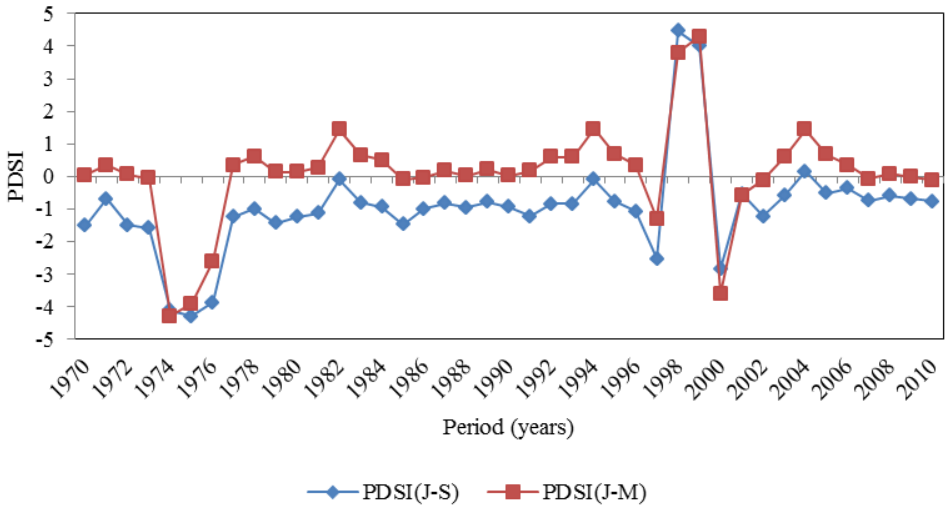

Figure 7. Time series of PDSI for dry seasons at Naro-Moru meteorological station.

(PDSI=-0.400) droughts are detected annually.

The rest of the months have positive PDSI values indicating wetness of different magnitudes in the river basin (Figure 9).

The area under extreme and severe droughts are 3758.01 (21.57%) and 1784.90 (10.25%) respectively for the year 1970 while the values for 2010 are 4540.36 (26.06%) and 2537.55 (14.57%) respectively as given in Table 6.

Spatially distributed drought severity based on PDSI

The results of spatially distributed drought severity based on PDSI show that the ranges of maximum and minimum drought severity values in 1970 are -0.868 to -0.804 and -0.675 to -0.610, respectively.

DISCUSSION

The spatial and temporal drought was found to significantly change for the period 1970 to 2010. The temporal variability of drought from 1970 to 2010 is described by negative values that indicate droughts of different severity and duration while the positive ones correspond to wet conditions. The findings indicate that extreme drought occurred twice in the four decades. It is

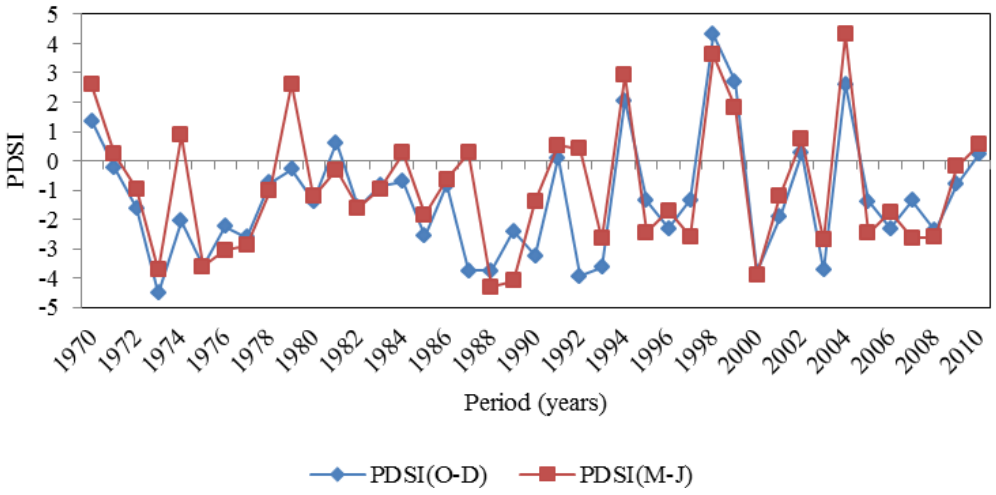

Figure 8. Time series of PDSI for wet seasons at Naro-Moru meteorological station.

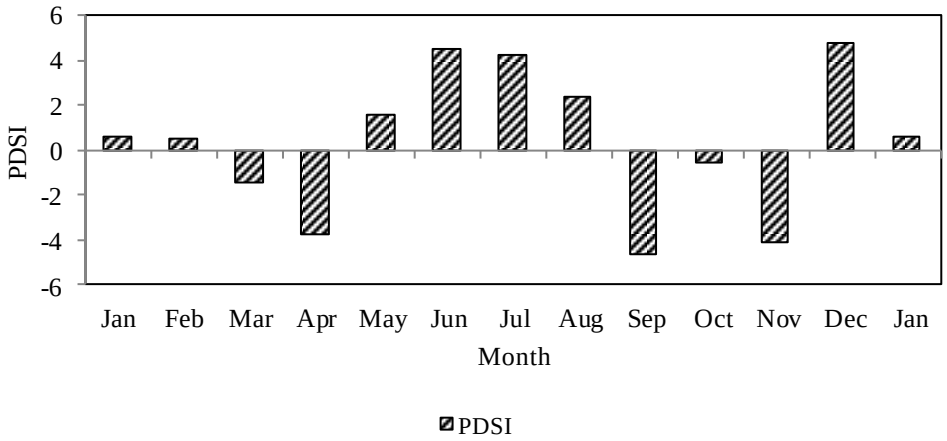

Figure 9. Monthly average PDSI for the period 1970 to 2010.

observed that for dry seasonal PDSI, the values in the months of January to March (J-M) are constantly higher than the ones for July to September (J-S). By comparing the time series PDSI values for dry and wet seasons for the meteorological stations, it can be seen that the time series plots for the PDSI values for dry season are generally lower than those for the wet seasons. The PDSI time series values for meteorological stations located at the lower elevation of the upper Tana River basin were lower than those for the stations which located at higher elevation. Thus, the PDSI results indicate that the areas within the lower elevations are more prone to drought risks than those in higher elevations. From the results of spatially distributed drought magnitude, there is a general increase in area under the extreme and severe drought as given by PDSI from 1970 to 2010. The distribution of extreme and severe drought categories dominate in the south-eastern parts of the upper Tana River basin while extreme wet and moderate wet conditions dominate the north-western areas. Thus, south-eastern parts of the basin have the highest risk of experiencing high drought magnitudes (Figure 10). However, the north-western areas have the lowest drought risks. Comparing the findings with similar research by Yan et al. (2013a; b) in Luanhe River basin, showed that the lowest PDSI values (PDSI< -4.00) are persistently observed in the north-western areas of Luanhe basin. On the other hand, the south-eastern areas of the upper Tana River basin exhibit similar lowest values of PDSI (PDSI< -4.00). The drought severity gave maximum and minimum drought severity values occurring respectively in the north-western and south-eastern areas of the basin. The maximum and minimum severity values increased from -1.478 to -1.348 and from -1.087 to -0.957 in 2010 as presented in the results. There was an increase in drought severity over the years of record (Figure 11). The trend in spatial PDSI severity values over time

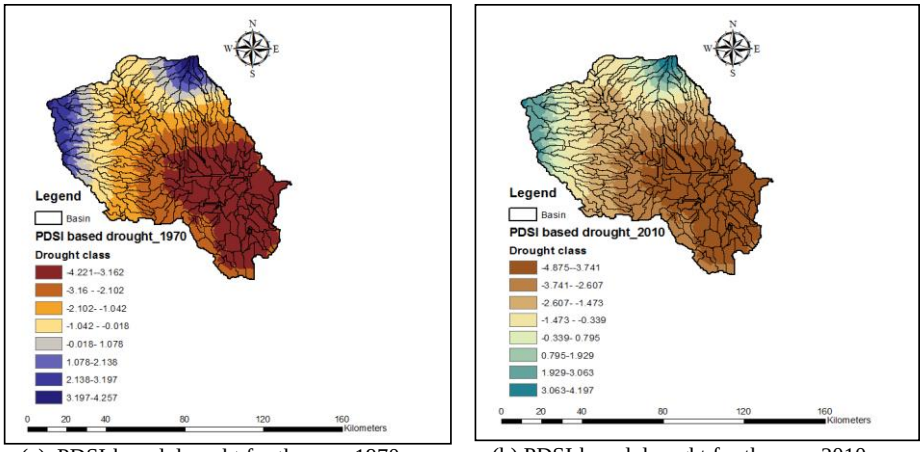

(a). PDSI-based drought for the year 1970 (b) PDSI-based drought for the year 2010

Figure 10. Spatially distributed magnitude of PDSI-based drought in October.

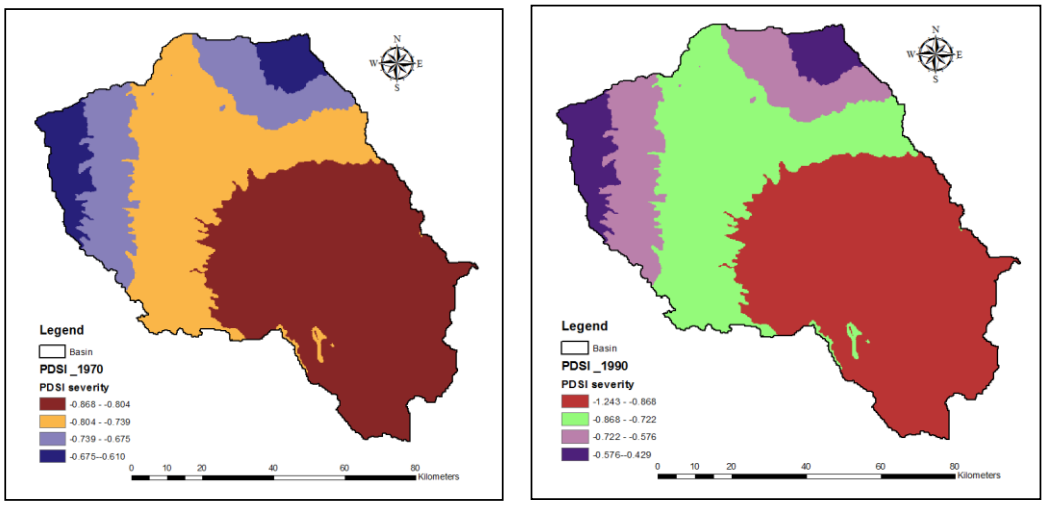

(a). Drought severity for 1970 (b) Drought severity for 1990

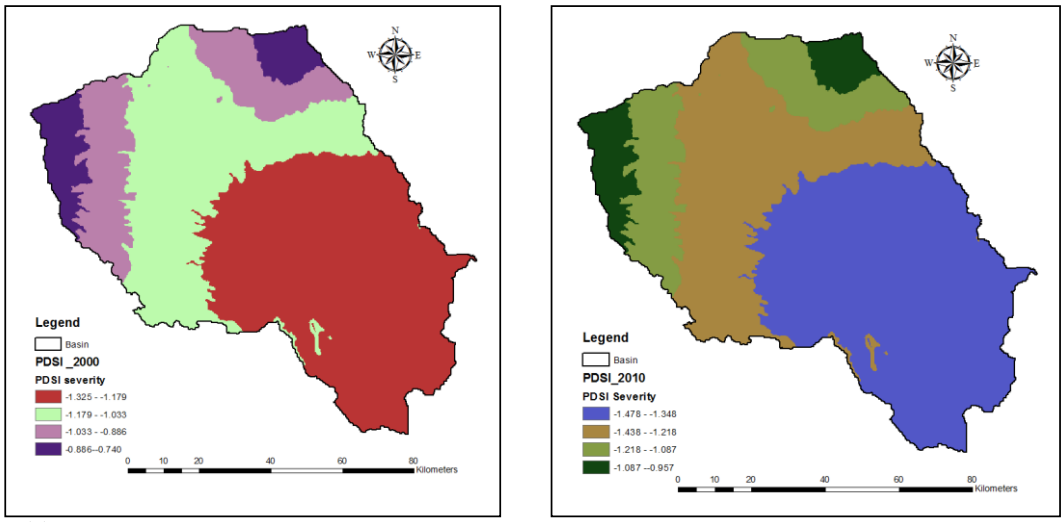

(c) Drought severity for 2000 (d) Drought severity for 2010

Figure 11. Spatially distributed PDSI-based drought severity.

compared closely with the spatial patterns trend explained as by Zoljoodi and Didevarasasl (2013). For instance, these authors showed that the PDSI severity values increased from -1.28 (1951-2005) to -7.68 (1999-2002) in Iran. In comparison with the present study, the results show that the PDSI increased from the range -0.675 to -0.610 in 1970 and from -1.087 to 0.957 in 2010 for the north-eastern areas of the upper Tana River basin. Thus, the findings can be used in decision making especially in prioritized drought mitigation measures within the river basin.

Conclusion

Spatial distribution of drought indicates that south-eastern parts of the basin are the most susceptible to droughts while the north-western areas are least prone to the droughts. From the results of spatially distributed drought magnitude, it can be seen that there is a general increase in area under the extreme and severe drought as given by PDSI from 1970 to 2010. The application of the PDSI reflects the spatial heterogeneity and temporal variability of drought across the upper Tana River basin. The drought assessment from this study offer technical approach for comprehensive understanding of drought for effective drought-induced disaster mitigation and its management, with a view to reducing adverse effects on livelihoods in the river basin. The findings show that the lowest PDSI values (PDSI< -4.00) are persistently observed in the north-western areas of upper Tana River basin. On the other hand, the south-eastern areas of the upper Tana River basin exhibit similar lowest values of PDSI (PDSI< -4.00). By comparing the time series results of PDSI for dry and wet seasons indicate that the temporal drought detected by PDSI values for dry season are generally lower than those for the wet seasons. The results of the study can be incorporated in drought early warning system and reduce adverse impacts of drought on water resources, ecosystems and peoples livelihoods.

CONFLICTS OF INTERESTS

The authors have not declared any conflict of interests.

ACKNOWLEDGEMENTS

The authors of this article appreciate the Egerton University, Division of Research and Extension for support in publication of this article. Great appreciation to the African Development Bank (AfDB) for scholarship offered for the PhD study that culminated to this paper. The authors are thankful to authors, editors and publishers of journals and books from where the literature of this article has been referred. The authors greatly appreciate the editorial board and the reviewers of the international journal of water resources and environmental engineering (IJWREE) for accepting to publish this paper and for the useful comments that improved the original manuscript.

REFERENCES

Barua S (2010). Drought assessment and forecasting using a non-linear aggregated drought index, PhD thesis, Victoria University, Australia.

Belayneh A, Adamowski J (2013). Drought forecasting using new machine learning methods. J. Water Land Dev. 18(I-IV):3-12.

Belayneh A, Adamowski J (2012). standard precipitation index drought forecasting using neural networks, wavelet neural networks and support vector regression. J. Appl. Comput. Intell. Soft Comput. 18(I-IV):3-12.

Bonal D, Burban B, Stahl C, Wagner F, Hérault B (2016). The response of tropical forests to drought-lessons from recent research and future prospects. Ann. For. Sci. 73:27-44.

Castano A (2012). Monitoring drought at river basin and regional scale: application in Sicily, PhD Dessertation in Hydraulic Engineering, University of Catania, Italy.

Hunink JE, Immerzeel WW, Droogers P (2009). Report on green water credits for the upper Tana River Basin, Kenya Phase II-Pilot operations biophysical assessment using Soil and water assessment tool SWAT.

IFAD (2012). Upper Tana catchment natural resource management project report, east and southern Africa division, project management department.

Jacobs J, Angerer J, Vitale J, Srinivasan R, Kaitho J, Stuth J (2004). Exploring the Potential Impact of Restoration on Hydrology of the Upper Tana RiverCatchment and Masinga Dam, Kenya, a Draft Report, Texas A & M University.

Karamouz M, Rasouli K, Nazi S (2009). Development of a hybrid index for drought prediction: case study. J. Hydrol. Eng. 14(6):617-627.

Karamouz M, Szidarovszky F, Zaharaie B (2003). Water resources systems analysis, Lewis Publishers, Florida, U.S.A

Karl TR, Knight RW (1985). Atlas of monthly palmer hydrological drought indices for the continuous United States, Asheville, N.C USA national climatic data centre, climatology series (3-7) report.

Loucks DP, van-Beek E (2005). Water resources systems planning and management, an introduction to methods, models and applications, studies and reports in hydrology, UNESCO publishing Paris.

Mishra AK, Singh VP (2010). A Review of Drought Concepts. J. Hydrol. 391(1-2):202-216.

Morid S, Smakhtin V, Bagherzadeh K (2007). Drought forecasting using artificial neural networks and time series of drought indices. Int. J. Climatol. 27(15):2103-2111.

Muchena FN, Gachene CKK (1988). Soils of the highland and mountainous areas of Kenya with special emphasis on agricultural soils, http: //wwwjstor.org, accessed on 25th May 2017.

Palmer WC (1965). Meteorological drought research paper 45, weather Bureau, Washington D.C, U.S.A.

Quiring SM, Papakryiakou TN (2003). An evaluation of agricultural drought indices for Canadian prairies. Agric. For. Meteorol. 118(1-2):49-62.

Sivaprakasam S, Murugappan A, Mohan S (2011). Modified Hangreaves equation for estimation of ETo in a hot and humid location in Tamilnadu state, India. Int. J. Eng. Sci. Technol. 3(1):592-600.

UNDP (2012). Kenya, adapting to climate variability in arid and semi-arid lands, project report on risks posed by climate variability to delivery of water framework directives, Environ. Int. in press.

Wang W (2010). Drought analysis under climate change by application of drought indices and copulas, MSc thesis in Civil and Environmental Engineering, Portland State University.

Wondie M, Terefe T (2016). Assessment of drought in Ethiopia by using self-calibrated Palmer Drought Severity Index. Int. J. Eng. Manage. Sci. 7(2):108-117.

WRMA (2010). Physiological survey in the upper Tana catchment, a

natural resources management project report, Nairobi.
Yan DH, Wu D, Huang R, Wang LR, Yang GY (2013a). Drought evolution characteristics and precipitation intensity changes during alternating dry-wet changes in Huang-Huai-Hai River basin. J. Hydrol. Earth Syst. Sci. 10:2665-2696.
Yan D, Shi X, Yang Z, Li Y, Zhao K, Yuan Y (2013b). Modified palmer drought severity index based on distributed hydrological simulation. J. Math. Problem Eng. 2013:1-8.
Zoljoodi M, Didevarasl A (2013). Evaluation of Spatio-temporal variability of droughts in Iran using Palmer Drought Severity Index and its precipitation factors through (1951-2005). *Atmos.* Clim. Sci. J. 3:193-207.

International Journal of Water Resources and Environmental Engineering

Related Journals Published by Academic Journals

- *International Journal of Computer Engineering Research*
- *Journal of Chemical Engineering and Materials Science*
- *Journal of Civil Engineering and Construction Technology*
- *Journal of Electrical and Electronics Engineering Research*
- *Journal of Engineering and Computer Innovations*
- *Journal of Engineering and Technology Research*
- *Journal of Mechanical Engineering Research*
- *Journal of Petroleum and Gas Engineering*

academicJournals